A novel biophysical quantum algorithm predicts super-conductive properties in animate and inanimate systems

Hans (J H) Geesink* and Dirk K F Meijer**

Abstract

This paper addresses the question whether superconductive phenomena in superconductive materials and in life systems have common physical grounds. An extensive literature survey was performed with regard to intrinsic energy gap frequencies reported on a range of superconductor materials as measured by different spectroscopic technologies. The registered frequencies were plotted on an acoustic scale and compared with earlier detected EM frequency patterns revealed in various life systems. A meta-analysis showed that the particular wave frequency patterns in superconducting materials have discrete coherent frequency bands and are very much in line with those found in biological systems. We hypothesize that the revealed individual frequencies either alone or in combination provide a means to select or identify materials that exhibit superconductive properties at elevated critical temperature ranges. We propose that the spectral energy gaps of superconducting materials can be positioned at the pointer states of a pattern of coherent frequencies, and can be described by an acoustic algorithm, coined by us the GM-biophysical principle. High Temperature Superconductors (HTSC's) show patterns of frequencies, in which frequency ratios of 2:3 (third harmonic) are incorporated in ratios of 1:2 (fundamental frequency). We propose to apply semi-conductive smectites (phyllosilicates), studied in detail by us earlier, that radiate GM-like EMF frequencies, in combination with HTC superconductor materials, to further improve superconductive properties as a modality of intrinsic quantum lasing. Our observations highlight a potential quantum bridge between superconducting properties in physics and biology.

Key Words: High temperature superconductivity, superconductors, macroscopic quantum properties, coherence/decoherence balance, fractal information networks, Bose-Einstein Condensate, BEC, Bardeen-Cooper-Schrieffer-theory, BCS-theory, Pythagorean-scale, polarons, polaritons, quantum biology, electromagnetic frequencies, meta-analysis in biophysics, toroidal model

***Quantum Biosystems* 2019; 10 (1): 1-32**

Introduction

In the present paper, an analysis has been made of the behavior of high temperature superconductors, and the possibility to order an EMF (electromagnetic field) frequency pattern of spectral energy gaps of semiconductors. This analysis touches upon the coherence theories about BEC (Bose Einstein Condensate), BCS (Bardeen Cooper and Schrieffer), and routes to design high temperature room temperature superconductors.

* Previous: Ir, Project leader mineral Nanotechnology, DSM-Research, the Netherlands** Em. Professor of Pharmacokinetics and Drug Targeting,University of Groningen, the Netherlands
Address: Groningen, Parklaan 17, 9724 AN, The Netherlands
e-mail: meij6076@planet.nl

The general concept of super-conductivity is that when certain metals are cooled to low temperature, the lattice becomes rigid enough to allow the coherent movement of vibrations called phonons. Since the lattice is positively charged, these vibrations can resonate with pairs of negatively charged electrons called Cooper pairs (**Figure 1**). These also form when the temperature drops below some critical threshold. It turns out that a phonon and a Cooper pair can together travel through the lattice with little or no resistance. This represents conventional superconductivity. However, as the temperature increases, the lattice begins to vibrate more strongly and at a critical temperature, the Cooper pairs break up and the superconductivity stops.

The measurement of this change at a critical temperature is one of the standard tests for superconductivity along with the measurement of zero resistance. BCS theory predicts that superconducting materials also expel any magnetic field, the so-called Meissner effect. This is another key test of superconductivity. The theory goes on to suggest that the material can expel fields only up to a certain strength. So there is also a critical field strength above which the material becomes an ordinary conductor again. Physicists have found all of these effects in conventional superconductors and they are now used as important tests of whether or not superconductivity has been observed. Many physicists think that BCS theory must somehow forbid superconductivity at temperatures above 160-200 Kelvin. And the observational evidence, until now, has certainly supported this view. Nobody has found a conventional superconductor that operates above these temperatures. But in fact, there seems nothing in the theory to prevent conventional superconductivity at much higher temperatures. (Cavalleri, 2017; 2018; Hu, 2014; Kaiser, 2014; Mourachine, 2004; Mitrano, 2016; Nicoletti, 2018; Okamoto, 2017; Zaanen, 2011).

Electronic excitations can transport energy and matter in the form of solitons, breathers, kinks or quodons with very different characteristics, which are discussed by Archilla (Archilla, 2018). They can transport electric charge, in which case they are known as polaron-breathers or solectrons. Nonlinear excitations can influence function and structure in biology at 310 K, as for example, protein folding (Meijer and Geesink, 2018a).

In crystals and other condensed matter, they can modify transport properties, reaction kinetics and interact with defects. Nonlinear excitations are inherent to Bose-Einstein Condensates, constituting an excellent framework for testing their properties and providing a pathway for future discoveries in fundamental physics (Archilla, 2018).
Davydov and Brizhik, earlier, proposed the bio-soliton model of superconductivity in organic materials (Brizhik, 1984). Later Davydov has used this bio-soliton model to explain the phenomenon of high-Tc superconductivity occurring in Cuprates (Davydov, 1988; Mourachkine, 2004). Also Laughlin argued that the strongly interacting electron matter of Cuprate superconductors is complex to a degree that approaches biology (Laughlin, 2005). The future of high-Tc superconductivity research may touch upon symmetry principles and scale invariance, taken into account that 'quantum criticality' may be caused by phase transitions driven by quantum fluctuations (Zaanen, 2011).

Recently, a hypothesis was proposed by Turner (Turner and Notalle, 2015 and 2016a), that emerging structures in biological systems, that exhibit macroscopic quantum properties, should also have increased critical temperatures in superconducting materials. It is known that coherence and entanglement are fundamental properties of quantum mechanics. These can be defined as the physical congruence of wave properties within wave packets and represent a property of stationary waves (i.e. temporally and spatially constant) that enable a type of wave interference, known as constructive. The authors conclude that quantum coherence with sufficient life-time is preserved in living cells at room temperature and suggest that coherent excitations arising in a biological system

are due to a coherent correlation among the phases of oscillations. We consider the possibility that such conditions can be mathematically described by the GM-scale biophysical principle (Geesink and Meijer, 2017a, 2018a).

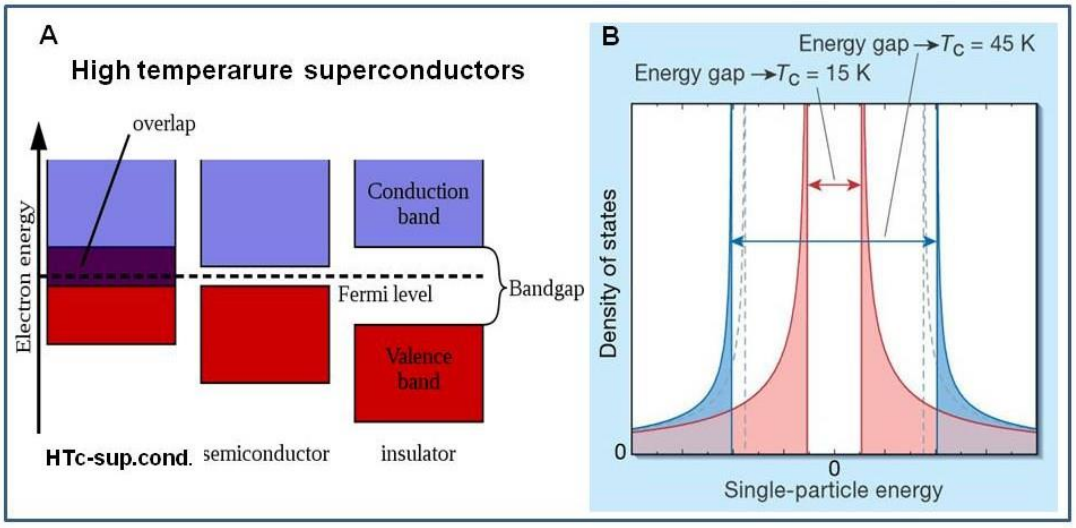

Figure 1: A. Bandgap and Fermi level of metal superconductors, semiconductors and insulators (ref. University of Queensland, 2011)

Interactions between particles/waves with a material lattice also facilitate thermalization, in which the particular phases can be considered as many-body localized (MBL) elements (Roushan, 2017) that can behave as stable solutions (Alet, 2018). The Bardeen-Cooper-Schrieffer BCS wave function can describe both the quantum state for Bose Einstein condensates (BECs) and superconductors (Byrnes, 2014). The similarity between the systems BEC and BCS can be understood by considering exciton-polaritons, and polarons. The exciton-polariton, formed in microcavities as a bosonic system, represent hybrid particles made up of photons strongly coupled to electric dipoles, and their presence demonstrates quantum coherent phenomena at high temperatures (Kavokin, 2010).

Polarons are the fermionic quasiparticles, produced by coupling of electrons and phonons in the presences of photons, that produce collective excitations of surrounding atoms/ particles. Both polarons and polaritons are supposed to be instrumental in promoting electron transport in suitable multi-layered materials (**Figure 2**).

In semiconductors, the intrinsic conductive gaps are small enough to be bridged by some sort of excitation. The gap is essentially some size "in-between" that of a conductor or insulator (**Figure 1**). In this model, a finite number of electrons is able to reach the conduction band and conduct small amounts of electricity.

The excitation of an electron also allows additional conduction processes to occur, due to the electron hole left behind. An electron from an atom that is close by, can occupy this space, creating a chain reaction of holes and electron movement that creates current. A small amount of doping material can drastically increase the conductivity of this material.

A crucial feature of super-conducting states is the abovementioned existence of energy gaps at the Fermi level region of the excitation spectrum. An energy gap is a region of suppressed density of states around the Fermi energy, in which the gap size represents the minimal energy that enables electron pairing (**Figure 1 and 2**).

The electron Cooper pairs form a coherent state in which the superconducting electrons have a lower energy than they would have in the normal state, enabling un-scattered wave travelling throughout the volume of the superconducting device (Ford, 2004). Probably de Broglie waves are responsible for the phase coherence.

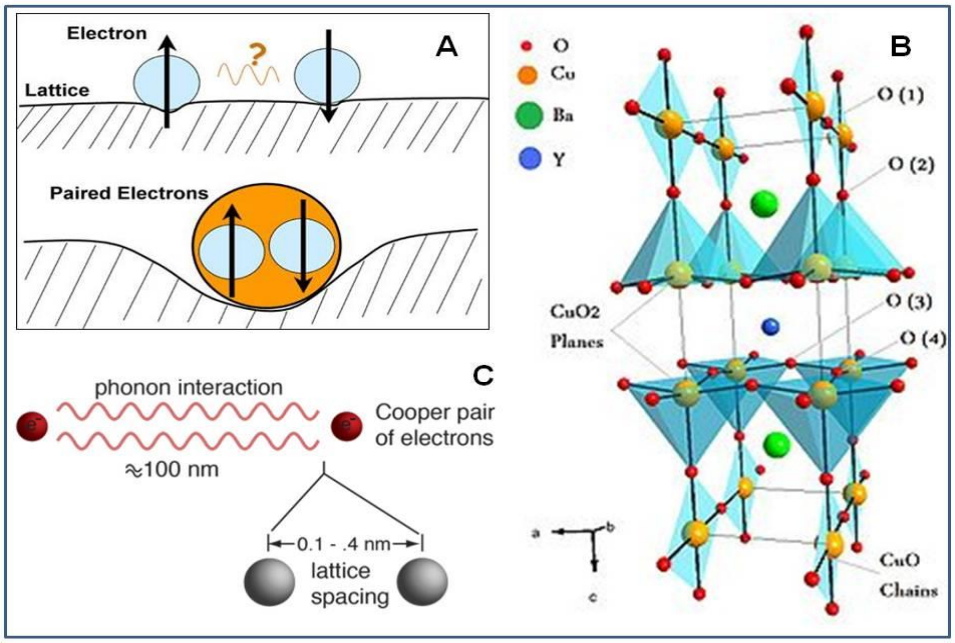

Figure 2: **A**: Phonon mediated lattice deformation produces cavity-facilitated pairing of Cooper-pair forming.
B: Long-distance Photon/Phonon excitation leads to delocalisation of oxygen atoms facilitating percolation if E-pairs through doped CuO2 materials C: Soliton wave passing a superconductive material, promoting intra-layer tunnelling/entanglement.

2. Possible mechanism of High-Temperature Superconductivity

An example of a high temperature superconductor is copper oxide (cuprate) ceramic doped with a variety of elements, from bismuth, yttrium and lanthanum to strontium and calcium.For still unknown reasons, this mélange of atoms conducts electricity without resistance at temperatures as high as 130 degrees above absolute zero (130 K or -143 degrees Celsius), unlike the conventional metallic superconductors that must be cooled below 20 K to become superconducting. (Wikipedia:High-Temperature superconductivity).

While conventional superconductors are explained by the seminal Nobel-Prize winning Bardeen-Cooper-Schrieffer (BCS) theory (Bardeen, 1957), high temperature superconductivity is still in search of a theoretical explanation. In the BCS theory, each electron pairs with an electron of opposite spin to form a new entity, a Cooper pair, that can move without resistance through the material. The pairing is made possible by interactions between the electrons and the metal atoms vibrating in place in the crystal lattice. The lattice is the ordered three-dimensional arrangement of atoms in a solid, like the scaffolding of a crystal.

The complex crystal structure of Bi-2212, a typical cuprate ceramic high temperature superconductor, shows two distinct alternating layers: the copper oxide layer (purple is copper, brown is oxygen) and the bismuth oxide layer (green is bismuth), interspersed with atoms of calcium (pink) and strontium (orange), see **Figure 2**.

A ceramic high temperature superconductor is actually a very poor metal, almost an insulator, at room temperature because electrons interact

only slightly with the solid lattice (top **Figure 2**), as represented by a slight depression in the crystal lattice. As the ceramic is cooled below a critical temperature, however, electrons pair up and are able to 'dance' with the vibrating lattice, stabilizing one another, as represented by a deep impression in the lattice.

Charge and spin orders in high-T_c cuprates and their interaction (and competition) with the superconducting state are believed to carry important information on the mechanism of high-temperature superconductivity. A prototypical case is that of the so-called “stripes” in the Cu-O planes of single-layer La-based compounds. These consist of one-dimensional chains of doped holes separating regions of oppositely phased anti-ferromagnetism, and this phase is typically stabilized by a distortion of the crystal lattice below a certain temperature (**Figure 2**). Most theoretical calculations, including phenomenological and diagrammatic approaches, converge on magnetic fluctuations as the pairing mechanism for these systems.

As also treated above, in a superconductor, the flow of electrons cannot be resolved into individual electrons, but instead consists of many pairs of bound electrons, called Cooper pairs. In conventional superconductors, these pairs are formed when an electron moving through the material distorts the surrounding crystal lattice, which in turn attracts another electron and forms a bound pair. This is sometimes called the "water bed" effect (**Figure 2**). Each Cooper pair requires a certain minimum energy to be displaced, and if the thermal fluctuations in the crystal lattice are smaller than this energy the pair can flow without dissipating energy. This ability of the electrons to flow without resistance leads to superconductivity.

An implicit assumption is that superconductive properties can be treated by mean field theory (Wikipedia: High Tc super-conductivity). In addition to the superconductive gap, there is a second gap. If the density of states is suppressed near the Fermi energy but does not fully vanish, then this suppression is called pseudogap. Pseudogaps are experimentally observed in a variety of material classes; a prominent example are the cuprate high-temperature super-conductors.

In superconductors type 2, the cuprate layers are insulating, and the superconductors are doped with interlayer impurities to make them metallic (**Figure 2**). The super-conductive transition temperature can be maximized by varying the dopant concentration (see appendix 1). The simplest example is La(2)CuO(4), which consist of alternating CuO(2) and LaO layers which are insulating when pure. When, for instance, 8% of the La is replaced by Sr, the latter act as dopants, contributing holes to the CuO(2) layers, and making the sample metallic. The Sr impurities also act as electronic bridges, enabling interlayer coupling.

With this realistic picture of the electronic and atomic structure of high temperature superconductors, one can show that the basic pairing interaction is still interaction with phonons, just as in the type1 metallic superconductors with Cooper pairs. While the undoped materials are antiferromagnetic, even a few % impurity dopants introduce a smaller pseudo-gap in the CuO2 planes which is also caused by phonons (technically charge density waves).This gap decreases with increasing charge carriers, and as it nears the superconductive gap, the latter reaches its maximum. The central question with regard to high temperature superconductivity, is why are the transition temperatures so high?

The **weak coupling theory** suggests superconductivity emerges from anti-ferromagnetic spin fluctuations in a doped system. According to this theory, the pairing wave function of the cuprate HTS should have a *d*x2-y2 symmetry. Thus, determining whether the pairing wave

function has *d*-wave symmetry is essential to test the spin fluctuation mechanism.Similar models can be made for iron-based superconductors but the different material properties allow a different pairing symmetry.

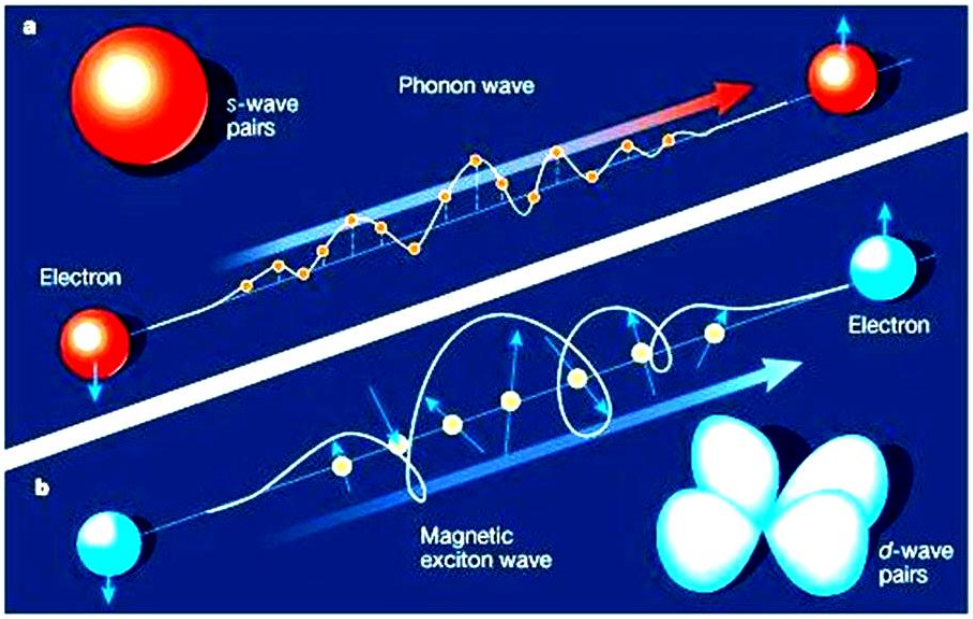

Figure 3: The influence of magnetic excitation waves (below) and phonon wave excitation on d -wave and s-wave electron pair formation. Electron transport, bearing a magnetic component is leading to p-wave pairs or (above) to s-wave pairs through interaction with phonon waves (charge density lattice vibrations)

Secondly, there is the **interlayer coupling model**, according to which a layered structure consisting of BCS-type (*s*-wave symmetry) superconductors can enhance the superconductivity by itself. By introducing an additional tunnelling interaction between each layer, this model successfully explained the anisotropic symmetry of the order parameter as well as the emergence of the HTS. There have been numerous experiments such as photoemission spectroscopy, NMR, specific heat measurements, but the results were ambiguous, some reports supported the *d* symmetry for the HTS whereas others supported the *s* symmetry (**Figure 3**).

Thirdly in a **two-band model** Kruchinin the transition temperature becomes higher than that derived within a single-band model, because of the tunneling of Cooper pairs between two bands. Phase diagrams for the two-band superconductivity has been calculated and the tunneling of Cooper pairs causes stabilization of the order parameter of the superconductivity (Kruchinin, 2016).

Potential of Photon Lasing-induced Superconductivity and spin-type ordering

The emergence of coherent interlayer transport at temperatures as high as 20 K has been demonstrated via time-domain THz spectroscopy, by *detecting a Josephson Plasma Resonance* in the transient c-axis optical reflectivity (Cavalleri, 2017; 2018). High-energy (1.5 eV) photo-excitation can strongly enhance the interlayer superconducting coupling in striped compounds, in particular for pump polarization perpendicular to the CuO_2 planes The most striking results on high-T_c cuprates were achieved on the well-known **bi-layer compound** $\mathbf{YBa_2Cu_3O_{6+x}}$,which has a maximum critical temperature at equilibrium $T_c \simeq$

90 K. By using mid-infrared pulses to induce large-amplitude modulations of the lattice (and in particular of the position of the so-called apical oxygen atoms), local vibration modes can be improved (**Figure 4**). The mutual feedback of the magnetic and electron-phonon interaction is critical to the high temperature superconducting state. There is pairing in the two populations of electrons, one "localized" and the other "free," both perhaps enhanced by the electrons' interactions with the crystal lattice. If the localized electron pairs are bound lightly enough to the lattice atoms, they can resonate with the coherent motion of the Cooper pairs of free conducting electrons, leading to superconductivity.

There are materials where the electron-phonon interaction enhances a spin type of ordering and vice versa. This has not been observed before in high temperature superconductors. The formation of the electron pair, the Cooper pair, is mediated through the phonons, and at the same time there is a feedback from the magnetic interaction. So, the two enhance one another (Cavalleri, 2017). In high temperature superconductors, the repulsive electron-electron interaction is very strong, and the tendency for electrons of opposite spins to pair up into a "singlet" is probably related to the anti-ferromagnetic interaction that's responsible for making the undoped ceramic materials anti-ferromagnets.

However, it is generally believed that this tendency to form spin singlets enhances the interaction between the electrons and the phonons, (**Figure 5 and 6**).

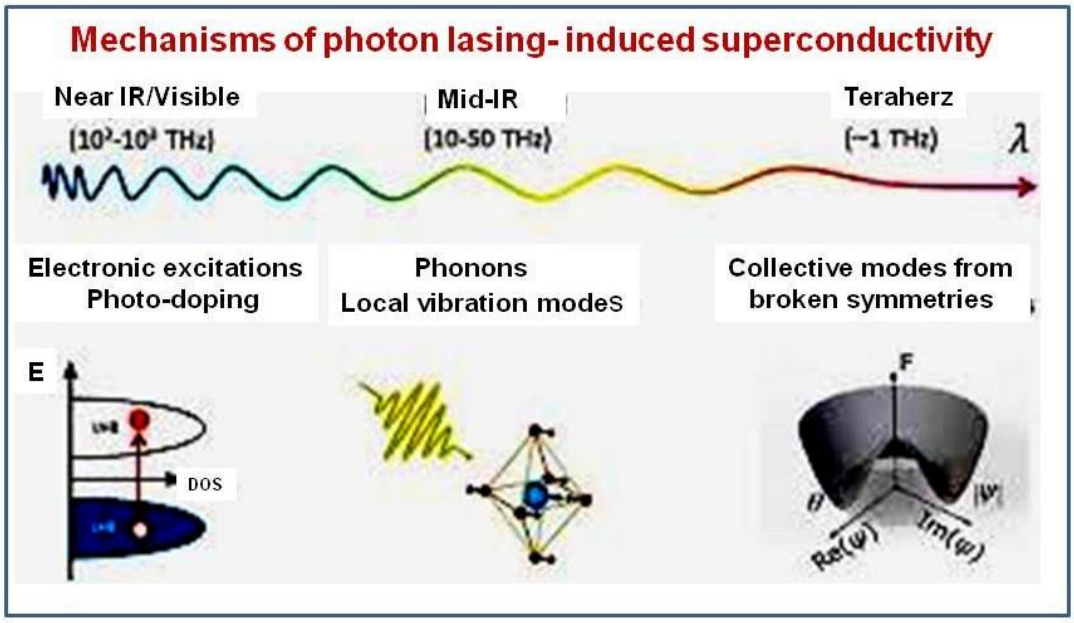

Figure 4. Energy scales of the fundamental excitations of solids in the visible and infrared EM spectrum. Whereas, light pulses at near-infrared and visible frequencies (10^2–10^3 THz) drive electronic transitions, phonons and other collective modes can be excited at MIR and THz frequencies (Modified from Cavalleri, 2017)

Qualitative explanation of the spin-fluctuation mechanism

In a high-Tc superconductor, the mechanism is similar to a conventional superconductor. In this case, phonons may play a secondary role, being assisted by spin-density waves. Just as all known conventional superconductors are strong phonon systems, all known high-Tc superconductors are strong 3D spin-density wave systems, within close vicinity of a magnetic transition. When an electron moves in a high-Tc superconductor, its spin creates a spin-density wave around it.

This spin-density wave in turn causes a nearby electron to fall into the spin depression created by the first electron.

Hence, again, a Cooper pair is formed. When the system temperature is lowered, more spin density waves and Cooper pairs are created, eventually leading to superconductivity. However in high-Tc systems, as these systems are magnetic systems due to the Coulomb interaction, there is a strong Coulomb repulsion between electrons. This Coulomb repulsion prevents pairing of the Cooper pairs on the same lattice site. The pairing of the electrons occur at near-neighbour lattice sites as a result. This is the so-called d-wave pairing, where the pairing state has a node (zero) at the origin.

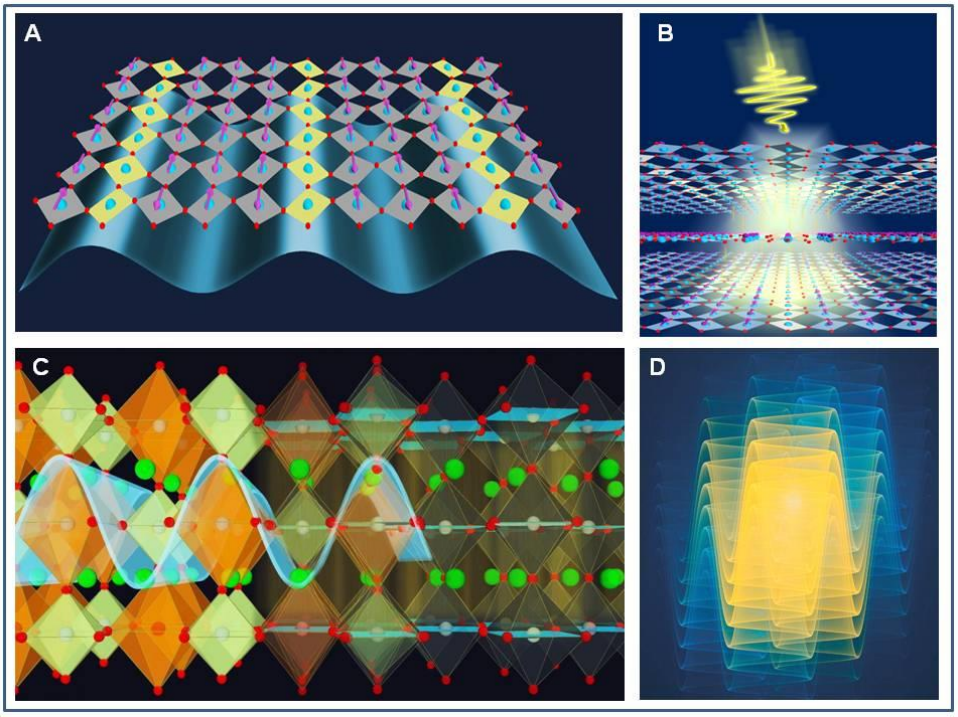

Figure 5: **A**. Schematic drawing of charge, spin, and lattice arrangement within a CuO2 plane (Cu blue, O red spheres) in the stripe-ordered LTT phase. Holes form stripes (yellow) which separate domains of oppositely phased antiferromagnetism **B**: Side view of a layered Cuprate like $La_{1.675}Eu_{0.2}Sr_{0.125}CuO_4$ exhibiting one-dimensional "stripes". By photo-exciting one such non-superconducting striped compound with mid-infrared pulses, it can be transiently transformed into a superconductor within few picoseconds **C**: Cartoon of soliton wave passing a superconductive material, promoting intra-layer tunnelling/entanglement. **D**: Cartoon of fractal soliton wave (modified from Cavalleri, 2018)

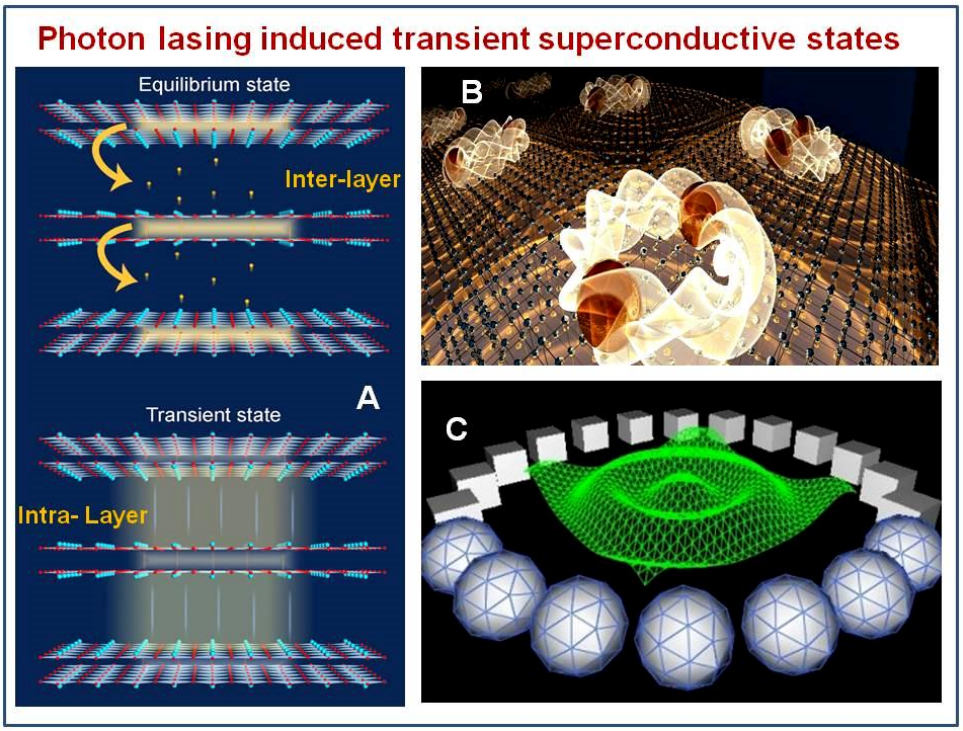

Figure 6: **A** pulsed photon lasing produces a shift in inter-layer connection of coherent condensates to improved intra-layer conductivity; **B**: Rotational (spiral) architecture of superconductive materials invites toroidal generation of photon/electron and phonon/ electron quasi particles; **C**: Collective coherent mode of macro-vibrations in the superconductor matrix can be produced by information collected in toroidal trajectories (blue spheres) in interaction with discrete wave frequencies derived from zero-point energy stored information. This on the basis of stochastic electrodynamic principles assuming pilot wave steering (depicted by cubes)

Third harmonic susceptibility probes the superconducting transport processes

HTSC's show patterns of frequencies, in which frequency ratios of 2:3 (third harmonic) are incorporated in ratios of 1:2 (fundamental frequency). A manifestation of electron-hole pairing as a nonlinear electromagnetic response of layered superconductors show that the pairing causes the appearance of a number of peaks in the frequency dependence of the intensity of the third-harmonic generation (Germash, 2017; Cea, 2018; Gioacchino and Bianconi, 2010). The highest peak corresponds to $\hbar\ \omega\ = (2/3)\ \Delta$, where ω is the incident wave frequency, and Δ is the order parameter of the electron-hole pairing (Germash, 2017).

For samples with three-dimensional superconductivity, the superconducting signature can be seen at both the fundamental frequency and at the third harmonic. By driving the system out of equilibrium with an intense infrared light at a typical frequency, a net coupling between the layers is induced, and the superconducting signature shows up in the third harmonic (Tranquada, 2018; Rajasekaran, 2018).

3. Smectite minerals as potential superconductor

One of us (H. Geesink) performed research on the potential semi-conductive properties of phyllosilicates (mineral nanotechnology of highly purified clay materials) (Geesink, 2007). One example of such material is called smectite (see structure in **Figure 7**). The structure of smectite, being an example of the family of phyllosilicates, resembles a sort of mica structure, in that it has an octahedral sheet in coordination with two tetrahedral sheets in which oxygen atoms are

shared. Cationic substitution occurs in octahedral or tetrahedral sheets, and the corresponding differences in properties and chemical composition are used to classify the smectites (Borchardt, 1977; **Figure 2**). Mica muscovite shows stationary and moving breathers that represent localized nonlinear excitations with an internal vibration (Archilla, 2015).

Smectites make use of comparable structures as high-temp Cuprate ceramics, containing iron like the iron-based superconductors, and in addition many other dopants. Fripiat (1982) reported the relationship between the frequencies of these dopants and √(z/m), where z and m are, respectively, the charge and the mass of compensating cations of these smectites. Smectites show chiral properties present as parity-violating weak interactions in the crystalline enantio-selective structure (Tranter, 1985).

A dynamical model of the propagating nonlinear localized excitations, in the cation layer in a mica muscovite has been developed, in which supersonic kinks can propagate (Archilla, 2015).

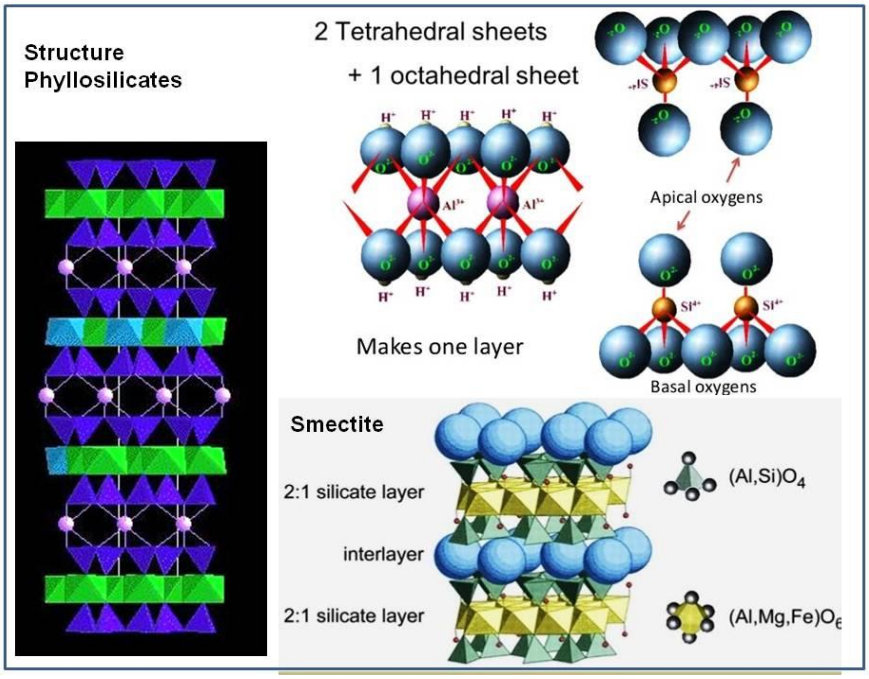

Figure 7: Clay minerals (phyllo-silicates and smectite nano-structures)

Smectites show a macroscopic 3D-laminar multi doped ordered structure like HTSC's and are able to generate typical energies, that are in resonance with 3D-atomic structures at IR vibrations, and electronic transitions in a very broad range of typical coherent frequencies at UV, Visible, NIR, MIR, FIR, and GHz (see later sample 20). The frequencies of the electromagnetic spectrum show patterns of ratios of 1:2 and 2:3 (Coyne, 1985; Geesink and Meijer, 2017a; 2018b).

4. Superconductivity in living systems

A relation between high-temperature superconductors and the ordering of living matter has earlier been proposed by Vasconcellos (2012), and Poccia (2011a,b), as well as in the theory of Fröhlich (1968). The central item here is that a particular wave-information is able to affect living cells at frequencies in the surrounding of a thermal bath, in which a large numbers of quanta

condense into a single state. The latter has been tentatively defined as a Bose-Einstein condensate, and is supposed to induce physical and non-thermal interactions between bio-molecules.
The waves can take dimensions that are many orders of magnitude larger than that of the microscopic objects, due to the fact that the resulting overall wave field is highly correlated, and therefore has an analogy with the behavior of high temperature superconductors (Jerman, 2016).

In the present paper it is postulated that typical coherent frequencies in superconductors resemble that of the living cells/biomolecules and can be described by a wave equation of coherence, that also describes the degree of entanglement and semi-harmonic distribution of particle physics (see section 5) and have a relation with Smectite minerals.

It is also known that in redox reactions occurring in living organisms, electrons are transferred from one molecule to another in pairs with opposite spins; and electron transport in the synthesis process of ATP (adenosine triphosphate) molecules in conjugate membranes of mitochondria and chloroplasts is realized by pairs, but not individually (Davydov, 1990; Mourachkine, 2004)

It happens that in inorganic solids two electrons, in some circumstances, can be paired too. This is particularly true in the case of high-Tc superconductivity (Mourachkine, 2004). Even before the discovery of superconductivity in organic salts, Davydov has shown that, in some biological processes, the quasiparticles in living tissues are paired. Soon after the discovery of superconductivity in organic compounds in 1979, Davydov and Brizhik proposed the bio-soliton model of superconductivity in organic materials (Brizhik, 1984).

Later, he has used the bio-soliton model to explain the phenomenon of high-Tc superconductivity occurring in Cuprates (Davydov, 1988; Mourachkine, 2004).

Thus, the two processes seem to be related, and if this is experimentally confirmed, this can lead to a better understanding of the phenomenon of superconductivity in solids in general.

As mentioned earlier, Turner and Notalle, (2016a) reported on recent theoretical developments, which suggest that a set of shared principles underpin macroscopic quantum phenomena observed in high temperature superconducting materials, room temperature coherence in photosynthetic processes and the emergence of long-range order in biological structures.

These systems are driven by dissipative systems, which lead to fractal assembly and a fractal network of charges (with associated quantum potentials) at the molecular scale.

At critical levels of charge density and fractal dimension, individual quantum potentials merge to form a ‘charged-induced’ macroscopic quantum potential, which act as a structuring force dictating long range order.

Whilst the system is only partially coherent (i.e. only the bosonic fields are coherent), within these processes many of the phenomena associated with standard quantum theory are recovered, with macroscopic quantum potentials and associated forces having their equivalence in standard quantum mechanics.

They established a hypothesis that the development of structures analogous to those found in biological systems, should lead to increased critical temperatures in high temperature superconducting materials, very much supporting our view on similarities between discrete frequency patterns in both superconductors and life systems as found in the present study.

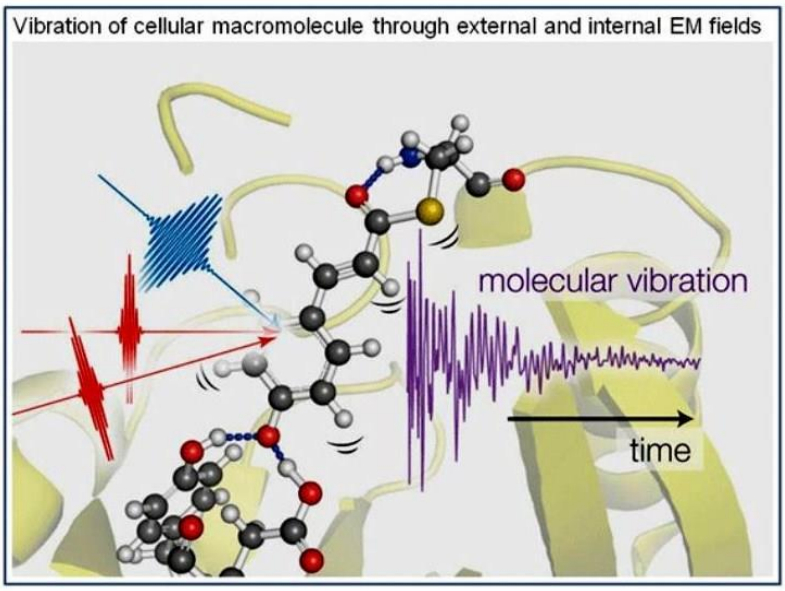

Figure 8: Internal (blue arrow) and external(red arrows) EM-fields with discrete wave frequencies influence the 3-D structure and vibratory states of macromolecules in life systems.

The biophysical GM-scale algorithm even enables a prediction of which eigenfrequencies of non-thermal electromagnetic waves that are life-sustaining and which are, in contrast, detrimental for living cells.

The particular effects are exerted by a range of electromagnetic wave eigen-frequencies of one-tenth of a Hertz till Peta Hertz that show a pattern of 12 discrete bands, and can be positioned on an acoustic reference frequency scale (Geesink and Meijer, 2017a). This typical quantum wave interference pattern is likely to be based on the features of semi-harmonic oscillators as treated in the following section.

5. Semi-harmonic quantum oscillators and influence of zero-point energy

A quantum harmonic oscillator equation is mostly used to describe coherent processes in quantum mechanics related to quantum entanglement and is a quantum-mechanical analog of a classical harmonic oscillator (see Wikipedia: Quantum harmonic oscillator). An arbitrary potential can be approximated as a harmonic potential in the vicinity of a stable equilibrium point. It is one of the few quantum-mechanical systems for which an exact, analytical solution is known, see **Fig. 9**.

In this model the energies are quantized, meaning that only discrete energy values (integer-plus-half multiples of $\hbar\omega$) are possible. The lowest achievable energy (the energy of the n = 0 state) is called the ground state and is not equal to the minimum of the potential well, but $\hbar\omega/2$ above it, and is called the zero-point energy. The harmonic oscillator eigenvalues of energy levels for modes ω_k are $E_n = (1/2 + n)\ \hbar\omega_k$, and when the zero-point energy is ignored then the levels are evenly spaced.

In a study of Turner and Notalle, 2016b on self-organization in plants they stated: “It appears that as a molecular scale fractal structure evolves, it reaches a critical point, resulting in the emergence of nm-scale structures.

This smaller scale of assembly may be explained by van der Waals forces playing a synergistic role alongside the macroscopic quantum potential at the nm-scale.

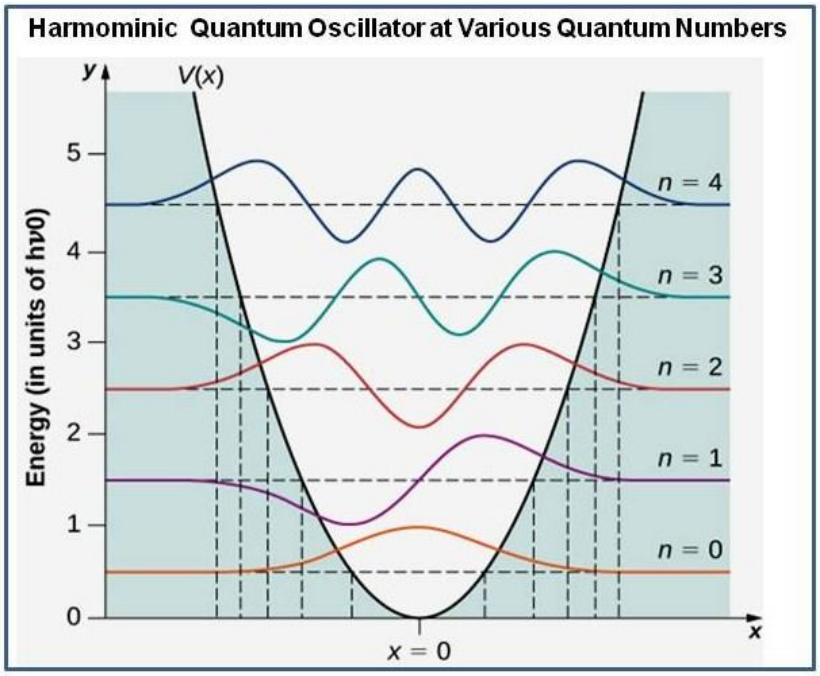

Figure 9. Example of an harmonic quantum oscillator: the general solution to the Schrodinger equation leads to a sequence of evenly spaced energy levels characterized by a quantum number n; depicted n = 1, 2, 3, and 4.

A more speculative, additional explanation lies in a second synergistic (attractive) quantum potential originating from Casimir forces, associated with the quantum vacuum itself. For a detailed treatment of this topic we refer the reader to theoretical studies by Simpson (2015) and references therein. Simpson's thesis suggests that Casimir forces cannot be considered in isolation in an inhomogeneous medium. Relating the ideas developed by Simpson to our approach, the electromagnetic field associated with the quantum vacuum is fundamentally coupled to the fractal molecular scale medium, with quantization of the coupled system creating polaritons".

The authors Turner and Notalle (2015) state that the assembly of molecular scale fractal networks is driven by a combination of quantum vacuum and thermal fluctuations acting as a sea of harmonic oscillators in combination with charge-induced repulsive forces between adjacent charged particles, which influence the dynamics of molecular assembly.

They also refer to a "missing force" related to quintessence-like behavior (dark energy/zero-pont energy scalar field), leading to a concept of collective macroscopic quantum forces that plays a critical role in the emergence of biological structure within the theory of scale relativity. It is known that the vibrational potential energies vary if its particle/wave distances change and are not evenly spaced. Therefore, a more practical relationship is proposed, called: "approximately harmonic over small oscillations" about an equilibrium, in which anharmonic behavior plays a clear role and can be described as a perturbation of a single-particle harmonic oscillator (Lane, 2017, **Figure 9**).

6. Short summary of our previous work.

Our previous analysis of about 500 articles from 1950 to 2017, dealing with endogenously measured and exogenously applied EM field frequencies in tissues, cells and biomolecules, revealed coherent

patterns of beneficial biological effects related to electromagnetic waves on in vitro and in vivo life systems, and could be positioned in the sub Hertz till Peta Hertz range into the Pythagorean-scale. Frequencies just in between the beneficial frequencies (defined as non-coherent) were shown to be related to patterns of detrimental biological properties, (Geesink and Meijer, 2018a,c).

The detected eigenfrequencies could be arithmetically scaled according to an adapted Pythagorean tuning and the semi-harmonic scale exhibits a core pattern of twelve eigenfrequency functions with adjacent self-similar patterns, according to octave hierarchy (Geesink and Meijer, 2018a). All pointer states related to the coherent behavior can be described by the proposed "coherence equation", coined by us the generalized (GM) biophysical principle. Importantly, a very similar distribution pattern of EM frequencies could be found for entangled conditions in Einstein–Podolsky–Rosen experiments, that show quantum entanglement of particles/waves (Geesink and Meijer, 2018b) as well as in the energy distribution of the entire range of elementary wave/particles in the standard model (Geesink and Meijer, 2018c).

In general, it was concluded that the particular algorithm is valid for both animate and a spectrum of inanimate systems, and therefore a general biophysical principle could be implied (Meijer and Geesink, 2018 a).

A coherence equation has earlier been proposed by us, that is able to describe coherent waves, in which harmonic and anharmonic excitations are integrated, and is called a semi-harmonic quantum oscillator. The equation describes distributions of 2/3 ratio's in 1/2 ratio's and approaches thereof and has been based on an adapted Pythagorean tuning.

The zero-point energy is proposed to be located in this equation at THz-frequencies, and decoherent oscillations are described by a second equation, in which the frequencies are logarithmically positioned just in between the coherent frequencies (Geesink and Meijer, 2018a,b).

The discrete standing wave pattern of EM wave frequencies can be mathematically expressed in a "quantum entangled wave equation":

$$E_n = \hbar\, \omega_{ref}\, 2^n\, 3^m\, (2^p)$$

En : Energy distribution, ωref : Reference frequency 1 Hz,
$\hbar$: Reduced Planck's constant,
n : Series of integers: 0, 0.5, 2, 4, 5, 7, 8, -1, -3, -4,-6, -7,
m : series of integers: 0, 1, 2, 3, 4, 5, -1, -2, -3, -4, -5,
p : Series of integers: <-4, -4, -3, -2, -1, 0, 1, 2, 3, 4, 5, 6, > +52

The core pattern of twelve eigenfrequency functions with adjacent self-similar (fractal) patterns, according to octave hierarchy, resemble so-called pointer states being quantum states that are less perturbed by decoherence than other states. The particular environment allows them to exist almost as objectively as classical states and leave selected states essentially unperturbed (Zurek, 2008).

Potential cyclic/spiral/toroidal and periodic elements in superconductor space It is known from our previous work (Meijer and Geesink, 2016) that the intervals of this GM-scale can be described by a 3-D toroidal space model, as described by Amiot (2013). For example: the circle of "fifths" of the GM-scale can be positioned at rotoids (composed motions of rotations), that circles or spiralizes each sub-unit of the nested tori, together with inscribed triads, major-third and minor-third relations, see **Figure 10**.

Elementary cycles theory (ECT) of Dolce (2016), postulates that every elementary "particle" of nature is characterized by persistent intrinsic space-time periodicity.

In ECT the Planck energy spectrum is interpreted as an harmonic like spectrum of a mass-less periodic modalities of fundamental time

periodicity T (quantized energy: En= nhω = nh/T, discretized angular frequencies: nω, and time periodicity T = h/E).

According to 't Hooft (2007, 2016), it is assumed that a theory describing our world starts with postulating the existence of sub-systems that, in a first approximation, evolve independently, and then are assumed to interact. It is suspected that our world can be understood by starting from a pre-quantized classical or "ontological" system. If time would be assumed to be discrete, the Hamiltonian eigenvalues would turn out to be periodic. Both theories favor a quasi-classical and quantum ontological interpretation of quantum physics, as in a primary form earlier suggested by David Bohm, (1952), as discussed by us (Geesink and Meijer, 2018).

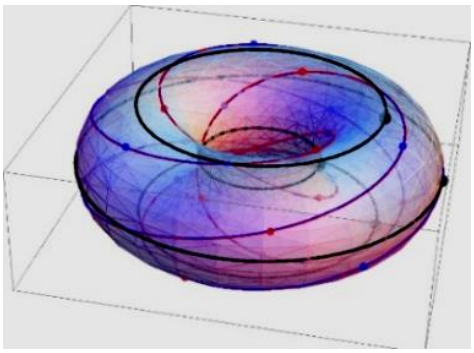

Figure 10. Triads, major, minor and augmented intervals positioned at rotoids, as composed motions of rotations, that circle a sub-unit of the torus, Amiot E. (2013).

Solitons/polarons, mentioned above, are a widely observed physical phenomenon that behave like solitary waves, but possess many features of particles. They are able to suppress anharmonicity (the deviation of a system from being a harmonic oscillator) by the excitation of high quantum levels, a process that facilitates the crossing of potential barriers and the transfer of a molecule to a new conformational state (Meijer and Geesink, 2018).

Particle attributes and particle conformation in space are linked, and knots can be scheduled as solitons (polarons), while toroidal solitons can be depicted as braids and framing. When particles within fields, move around following classical laws, than these classical laws could resemble classical field theories such as the Navier Stokes equations and the existence of vortex and toroidal solutions (Geesink and Meijer, 2018).

It is of interest in this framework that technology was developed to magnetically impose a collective toroidal fields within superconductive materials through ultra-compact double-spiral Nb resonators as used in (Averkin, 2013).

Also high-frequency quasi-periodic oscillations measured in a torus orbiting in the vicinity of a black hole probably obey to the Eigenfrequencies of the proposed algorithm. According to Rezzolla (2003), the torus, in fact, can be thought of as a cavity in which the p modes effectively behave as trapped sound waves. If the sound speed in the cavity were constant, the frequencies of these standing waves would be in an exact integer ratio. In reality the sound speed is not constant but the Eigenfrequencies found are in a sequence very close to 1:2:3:4. So cyclic energy trajectories and periodicity in quantum physics may be envisioned as recurrent spiral movements on a torus see **Figure 10**.

It is further proposed that Life Systems resemble typical coherent resonances of atomic cascade

transitions of materials used to show Einstein-Podolsky-Rosen's argument, and Bell's theorem that should be placed by a local realistic process in space-time. Potentially, these informational frequencies are linked with the zero point energy field, through resonances leading to phase-locked cellular information attractors, that are functionally separated by non-coherent wave activity (Keppler, 2016; Meijer and Geesink, 2018b).

The latter could explain the function of interwoven "coherent" EM/quantum values and the presence of trajectories corresponding with initial vibrational energies of molecules and atoms equal to their measured vibrational zero-point energy (Meijer and Geesink, 2018 b).

Measured spectral energy gaps of superconductors, normalized to a 12-number frequency scale

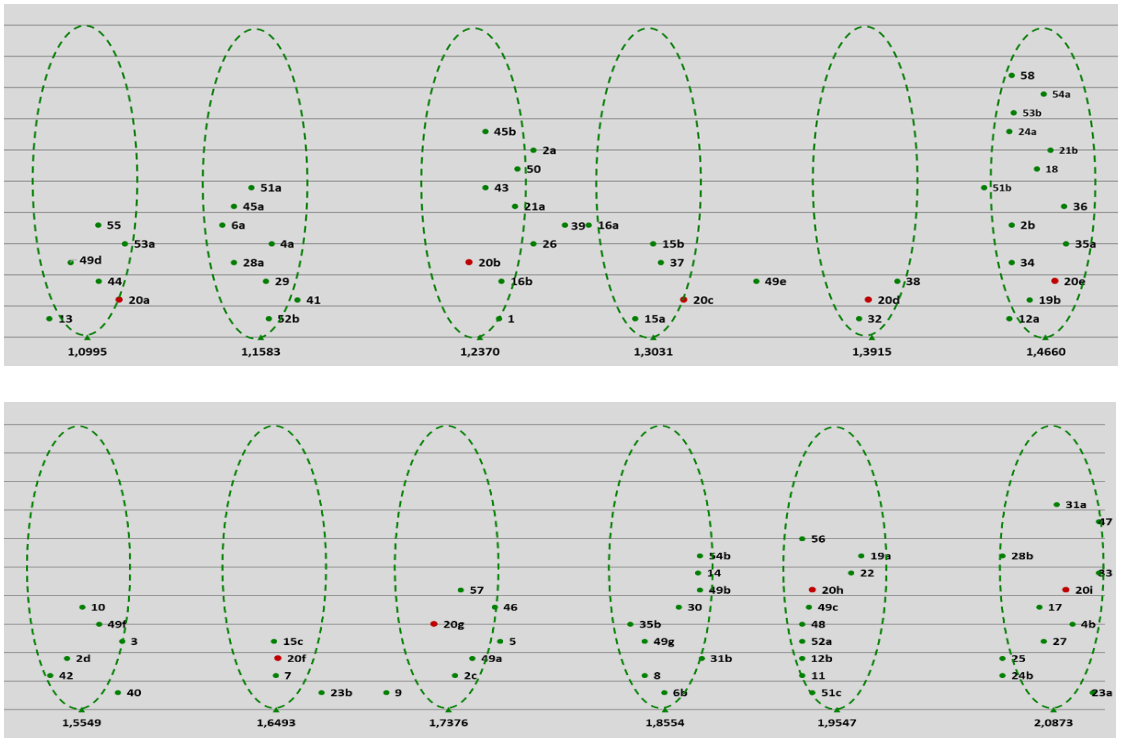

Figure 11. Pythagorean-normalized frequencies of spectral energy gaps of superconductors obtained from literature data and plotted on a logarithmic scale. Each point represents a single frequency value (on a reference quantum entangled THz-scale according to the proposed entangled quantum wave equation) and for clarity points are evenly spread out over the Y-axis; Labels depict the reference numbers of literature data and an experimental Smectite sample no. 20, in appendix 3.

Shi 2008 (1), Kouwenhoven 2017, 2018 (2a, 2b, 2c), Cardona 1987 (3), Cardona 1988 (4a, 4b), Thakur 2013 (5), Mohan 2006 (6a, 6b), Renk 1987 (7), Sugai 1987 (8), Xianyu 1990 (9), Ravindran 2003 (10), Kawano 1996 (11), Kawano-Furukawa 2002 (12a, 12b), Pickett 1994 (13), Zibold 1998 (14), Kadowaki 2008 (15a, 15b, 15c), Tafuri 2016 (16a, 16b), Homes 2000 (17), Paik 2011 (18), Reagor 2013 (19a, 19b), Geesink (2013) (20a, 20b, 20c, 20d, 20e, 20f, 20g, 20h, 20i), Kaiser 2012 (21a, 21b), Tan 2015 (22), Jin 2010 (23a, 23b), Qiu 2008 (24a, 24b), Zhou 2016 (25), Delfanazari 2018 (26), Bruér 2016 (27), Wei 2008, (28a, 28b), Okazaki 2014 (29), Jha 2014 (30), Bobrov 2006 (31a, 31b), Szczesniak 2015 (32), Chen 2013 (33), Ichimura 2008 (34), Saito 2012 (35a, 35b), Zhu 2013 (36), Jünger 2016 (37), Zhang 2017 (38), Charnukha 2015 (39), Shi 2008 (40), Schlesinger 1989 (41), Chen 1999 (42), Malaeb 2017 (43), Hong 2013 (44), Hüfner 2008 (45a, 45b), Li 2002 (46), Kim 2018 (47), Pavlosiuk 2015 (48), Semenok 2018 (49a, 49b, 49 c, 49 d, 49 e, 49 f, 49 g), Szczęśniak 2015 (50), Durajski (51a, 51b, 51c), Groll 2014 (52a, 52b), Sprau 2017 (53a, 53b), Nicoletti, 2017 (54a, 54b), Capitani, 2017 (55), Kizilaslan, 2017 (56). Ludbrook, 2015 (57), Manaf, 2015 (58).

7. Literature meta-analysis of spectral energy gaps of superconductors

The mean deviation of the 93 measured frequency data, relative to the calculated frequency data according to the 12-number scale, shows an accuracy of 0.76%, which is statistically significant (S.D on p=0.05 level).

This meta-analysis of the data of different superconductors gaps/frequencies from 1981 to 2018 reveals that the values can be positioned on EM pointer states and fit with the derived equation of coherent frequencies: an adapted Pythagorean-scale.

The discrete values of these frequencies have been positioned on a reference coherent TH-scale, that is expressed in twelve discrete coherent reference THz-frequencies: 1.0995, 1.1583, 1.2370, 1.3031, 1.3915, 1.4660, 1.5549, 1.6493, 1.7376, 1.8554, 1.9547, 2.0873 Thz (**Figure 11** and appendix 2). It has been shown that these spectral energy gaps of superconducting materials can be positioned at the pointer states of patterns of frequencies, that can be mathematically described by a deterministic quantum entangled wave equation.

The found correlation implies that there is a close relation with:

1) the entangled quantum states, shown in Einstein Podolsky and Rosen-experiments (Geesink and Meijer, 2018b)

2) quantum entanglement of elementary particles (Geesink and Meijer, 2018c), and with typical frequencies of living cells/biomolecules as revealed in the earlier studies (Geesink and Meijer, 2018a).

The proposed semi-harmonic code of nature, in the case of superconductors, shows precisely a frequency pattern as found for living cells and biomolecules from sub Hertz till PHz. This observation also confirms the concept that coherence in both life systems and inanimate systems can be described by a physical principle that guides quantum entanglement and has a relation with zero-point energy (Meijer and Geesink, 2016; 2018a).

This implies that the measured gap energies of superconductors fulfill local and non-local entanglement as described by the proposed physical principle. The highest critical temperatures of superconductors (Tc's in the range of 203-251 K, table 1 of appendix 3) are realized when multiple coherence peaks (energy gaps) are present, that obey to the quantum entangled wave equation (see samples nr. 49 and 51). The highest Tc's are realized between 4.5 and 9 meV at the THz-gap, that are in the band of Josephson plasmons.

8. General discussion

In our survey of intrinsic EMF frequencies in both type 1 and type 2 superconductors we found a distinct "band type" of frequency distribution on a normalized scale (**Figure 10**). This pattern, can be explained by a constructive quantum interference phenomenon and we postulated therefore that the superconductor matrix should be considered to have a quantized character and that quantum properties such as entanglement, and quantum tunneling should play a potential role. This makes it somewhat troublesome to talk about transport of particles such as electrons and quasi-particles such as polarons: instead one should envision a matrix of internal interacting wave fields.

As pointed out in our earlier studies (Meijer, 2015; Meijer and Geesink, 2018), both lattice and wave conditions are envisioned in a fractal structure of life systems being much in line with the recent proposals of Turner and Nottale (2015). Since fractality is by definition a continuum of self-similarity, the postulate of Turner et al that both quantum (at the micro scale) and classical aspects (at the meso- and macroscale) are at stake is open to question. This is very much related to

the conceptualization of space-time, that in case of a quantum system should be seen as also being *quantized*.

We argued earlier, in this respect, that space-time may be build up from energy vortices that connect through wormhole short cuts (Meijer and Geesink, 2018a), that even provides the known quantum foam modality at the Planck scale. It is also of interest that recently wormholes can be seen as instrumental in the attain superconductive properties in the framework of M-brane geometry (Seperhi, 2017), in which the wormhole structure can be interpreted as characteristic part of torus geometry. In a more generalized model, we postulated the geometry of the double torus as a basic building block of reality, implicitly introducing the potential of 4-D rotations.

In this respect a holographic feature is predicted in which the 3-D wave structure of superconductors is rather a shadow of a 4D-representation. The underlying AdS-Conformal Field Theory introduces the manifestation of gravity in the 4 D domain at the brink of 3D/4D space-time. Holographic superconductor models have been adequately reviewed (Horowitz, 2010; Rong-Gen, 2015).

This also focuses attention on the fact that any material superconductor is permanently embedded in a zero-point energy field. Consequently the intrinsic vibratory character of such fields should be taken into account as was realized in a number of previous papers on holographic aspects of superconductivity (Horowitz, 2010; Ron-Gen, 2015) as well as considerations on ZPE excitations (Turner and Nottale, 2016a).

It is important to note that in our earlier life studies a regular pattern of *both coherent and decoherent* frequencies were found. The coherent part of the GM-scale was defined by us as semi-harmonic since it is not only be based on integer numbers, as in classic harmonics, but also on imaginary (broken)numbers, according to an adapted Pythagorean scale, that imply a toroidal (rotational) aspect in the mathematical background.

Importantly, only coherent and no decoherent values were detected in the purely physical studies on entanglement and elementary particle studies as well as in the present superconductor studies. What could be the reasons that the decoherence aspect seems absent in the latter studies? Needless to say in the case of EPR and superconductors studies, this is likely to be due the selection of materials that have been made by the investigators in relation to an optimal function related to coherence and entanglement, yet, in principle, not excluding decoherent frequency values. Combinations of coherent and decoherent states according to the GM-scale, in principle would be found in all kind of atoms/molecules, and it may be that decoherent states are created through interactions in complex structures as an implicit feature.

We have earlier speculated that the combination of coherent and decoherent wave frequencies in the life systems could reflect a potential regulatory mechanism (Geesink and Meijer, 2017b; 2018d; Meijer and Geesink, 2018a). It has also been postulated that the balance of coherent and decoherent states may be more dynamic than earlier thought and that creation of a coherent or decoherent state by interaction with the environment, does not lead to information loss, and thus, in principle, could be a reversible process (Vatay, 2015). Consequently, it would be justified to think in terms of dynamic states of coherence/decoherence in a cycling mode (Meijer and Geesink, 2017; 2018a).

Life, including its quantum superconductivity, would thereby operate at the edge of chaos, in a so called poised realm, that allows the choice between two states in equilibrium, and thereby enabling fast responses essential for the cell ecology and survival.

Also, for instance, wave/particle duality may occur in a domain in which wave and particle modes are present at the same time. In fact, such a poised condition could be conceived as a thermodynamic balance between entropic and syntrophic (neg-entropic) aspects of reality. In fully physical systems such opposing conditions would have a more implicit character as for instance in matter/antimatter annihilation and forces such as gravity and dark energy. All this would imply a general aspect of symmetry and/or duality (Meijer and Geesink, 2018a).

The importance of both coherent and de-coherent aspects in mechanisms of super conduction was stressed by Turner and Nottale (2015): "One of the aspects of HTSC materials lies in their disordered structure, indicating that HTSC is favoured by complex fractal systems and that macroscopic quantum coherence phenomena such as HTSC is dependent on a *disordered* spatial distribution of charges/dopants/holes". A clear picture emerges that we need to understand HTSC in terms of the underlying physics of a *macroscopic quantum process*. Essentially one has to create the equivalent of a "complex path integral" in order to induce macroscopic quantum coherence.

We here propose that the disordered distribution in HTSC's is not a chaotic structure, but a partially rotational distorted structure, against the background of an ordered tetrahedral network structure, that thereby can be accommodated by toroidal geometry. The same complex structure has been found in Smectite minerals and in pure water molecules that are ordered in a partially distorted tetrahedral geometry (Geesink and Meijer, 2018e).

A crucial role for decoherent noise in superconductive biology has also be concluded from recent studies in quantum biology, in particular for the process of photosynthesis, (Engel, 2007; Collini, 2010; Romero, 2014).It was concluded that the wave character of particles allows excitons to pass through the plant matrix in a broad front, enabling an intracellular traffic of many parallel pathways that speed up the process of reaching the reaction centers.

However a second mechanism is involved to explain the high efficiency of this process: incoherent quantum noise of the conducting lattice facilitates a smooth passage of these charged units, in the process of energy transport (Plenio and Huelga, 2008, Huelga, 2013). A very similar concept on a crucial role of de-coherence processes (Turner and Notalle, 2015), was proposed in relation to superconductive modes, as mentioned above.

When energy levels reach a critical point, *destructive interference* effects (which we associate with observed quasiparticle interference in HTSC) will cancel out most frequencies, leaving those matching the resonant frequencies dictated by the geometry of the fractal network to form a complex velocity field and an associated macroscopic quantum potential (MQP), leading to the establishment of a coherent standing waves. We note that a very similar view on decoherence (taking a different approach and using different terminology) has been expressed by Dolce (2014) who consider gauge symmetry breaking in terms of the competition between quantum recurrence and thermal noise".

It is envisioned that the result of these processes will tend to exhibit a prominent coherent HTSC-system, fully guided by coherent wave domains, that can be described by toroidal geometry and numerically expressed by the GM-scale frequency pattern, as revealed in the present study. This implies that phonon- or photon lasing with the proper combination of coherent wave frequencies, decoherence is suppressed, leading to stable pointer states (*H. Geesink*). As an alternative, apart from this dominant influence of coherency in high-temperature superconductivity, some extent of decoherency may play a decisive role (see above) either by

matrix disturbances (vibrations) that may facilitate the overall rate of charge transfer, as have been suggested in recent studies on photosynthesis, or to fractal disordered selection of coherent spin states as suggested by Turner, while also the adding of general noise may promote the formation of polaron and polariton quasi-particles that, as mentioned before can be instrumental in Cooper-pair electron formation (**Figure 2 and 3**, *D. Meijer*).

9. Further research proposed

1) Entanglement and fractality can be further described by a geometry model of standing waves positioned on a torus geometry, as calculated by E. Amiot for musical scales using discrete Fourier transforms, see **Figure 10**, (Amiot, 2013). In the near future, we plan to complete the mathematical approach to further define the mathematical structures of the nested tori.

2) One of the keys to the high-temperature superconductivity is to improve the energy scales associated with the emergence of a coherent condensate of superconducting electron pairs. At the very basic level, what distinguishes the high temperature superconductors from the conventional superconductors is the fact that they are multi doped materials, of which the highly atomic-like 3d orbitals give rise to strong electron correlations, combined with elements that are weakly-coupled within two and three-dimensional layers. Experimental findings of superconductivity at 200 K in highly compressed hydrogen (H) sulfides, and rare earth atoms occupying the centers of the cages, have demonstrated the potential for achieving room-temperature superconductivity in compressed H-rich materials, that is closely associated with H clathrate structures with large H-derived electronic densities of states at the Fermi level and strong electron-phonon coupling related to the stretching and rocking motions of H atoms within the cages (Peng, 2017).

3) It is proposed to further investigate routes to achieve superconductivity approaching room temperature for typical Smectite-like minerals or new combinations of such materials. Sample nr. 20 is a Smectite-type, that shows multi energy transitions, that approaches the multiple 12 pointer states, that can be described by the GM-scale quantum wave equation (Geesink and Meijer, 2017b). This may be combined with external photon lasing if intrinsic wave energies of the smectites would require external coherent excitation. Interestingly, it have been shown recently by Nicoletti (2018), that application of external magnetic fields also can enhance interlayer phase correlation up to ten times, probably via activated tunnelling between optically-excited pair-density-waves.

4) High Tc superconductors are composite materials made of multiple structural modules of units and their electronic structure has multiple Fermi surfaces and gaps in the superconducting phase. Therefore, it is proposed to further investigate routes that make use of more than pentanary elements, preferably seven till nine, as has been pictured by Bianconi (Bianconi, 2012), see **figure 12**.

5) HTSC's show patterns of frequencies, in which frequency ratio's of 2:3 (third harmonic) are correlated to ratios of 1:2 (fundamental frequency).
A manifestation of electron-hole pairing as a nonlinear electromagnetic response of layered superconductors show that the pairing causes the appearance of a number of peaks in the frequency dependence of the intensity of the third-harmonic generation (Tranquada, 2018; Rajasekaran, 2018; Germash, 2017; Cea, 2018; Gioacchino, 2010).
It is wothtwhile therefore to further investigate the role of correlated frequencies at 2/3 and approaches thereof, as calculated by the GM-scale.

6) It is proposed to focus at higher Tc's positioned in the THz-gap between

4.5 and 9 meV, according to the analysis of the different superconductors.

7) If incoming (external) man-made electromagnetic signals indeed exhibit de-coherent EM radiation, than these signals, potentially, can decrease the overall coherency of (quantum) wave domains of living cells. A possible way to deal with such a problem is either to lower the energy density of the external man made de-coherent waves and/or to convert them to more coherent frequencies. We envision innovative methods for increasing the coherency of the electromagnetic signals through the use of appropriate semiconductor and superconductor technologies. Coherent terahertz waves, obeying to the GM-function, could be produced by appropriate semi-conductive and superconducting materials, inserted in electromagnetic man-made devices. This by making use of the knowledge with regard to the earlier mentioned Terahertz gap, through enabling the combination of supplied optical and electronic coherent information. Beneficial EM wave technology may therefore find applications by further improving health during the increasing use of EM-information/data in our society as well as in the design of therapeutic instrumentation for various chronic diseases and ageing processes (Geesink and Meijer, 2017b).

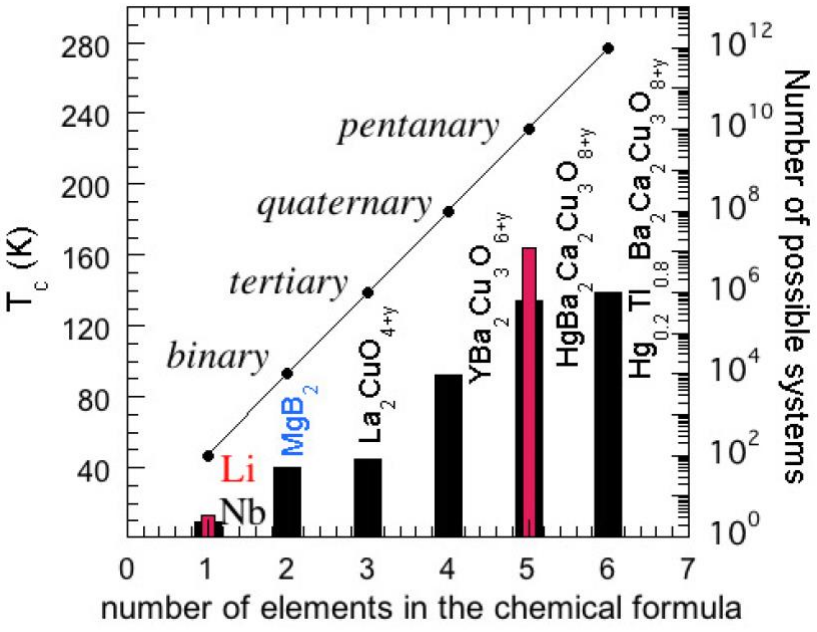

Figure 12. Number of elements in the chemical formula, picture of A. Bianconi and N. Poccia

10. Final conclusions

The found correlation between patterned frequency at approximate ratios of 2/3 in animate and non-animate systems in general (Meijer and Geesink, 2018a), is supported by the present close relation between the gap frequencies of the surveyed superconductors and the frequencies of living cells/biomolecules as also revealed our earlier studies. The proposed semi-harmonic code of nature, in the case of superconductors, shows precisely a frequency pattern as found for living cells and biomolecules from sub Hertz till PHz. This observation also confirms the concept that coherence in both life systems and inanimate systems can be described by a physical principle that mediates quantum entanglement and

also may have a relation with zero-point energy (Meijer and Geesink, 2016, Meijer and Geesink, 2018a). This implies that the measured gap energies of superconductors fulfill local and non-local entanglement as described by the proposed physical principle.

We infer therefore that high critical temperatures for superconductivity: T_c in the range of 203-251 K can be realized when the distribution of energy gaps can be described by the coherence equation (see for example sample nr. 49, and sample nr. 51). Smectites, sample nr. 20, have a potential for a study to pursue a proper operation at room temperature due to the fact that multi different energy transitions are located at multiple 12 different pointer states, described by the coherence equation. Phyllosilicates show also parity-violating weak interactions in the crystalline enantio-selective structure (Tranter, 1985), that is characteristic for a toroidal geometry pattern.

Coherent EM field frequencies according to the proposed quantum entanglement wave frequency, likely reflect beneficial solitons/polarons energies, which have been shown to be involved in macromolecular and cellular signaling similar to the formation of Bose-Einstein condensation as may also be related to superconductivity (Geesink and Meijer, 2017b; Meijer and Geesink, 2018a).

The hypothesis proposed by Davydov (1990) that the bio-soliton model explains the phenomenon of high-Tc superconductivity and the hypothesis of Turner and Notalle (2015, 2016a) and Laughlin (2005) that these superconductors are analogous to those found in biological systems are fully supported by the present results.

The present analysis of superconductor-data shows that a total of 93 independent measured spectral energy gaps in meV's of different superconductors match with coherent frequency assemblies of energy states located at the pointer states of a 12-number frequency quantum entangled scale as found for living cells and biomolecules. Superconductors with a high critical temperature can be found for materials that have *multiple* different energy transitions, that turned out to be precisely positioned at the proposed quantum entangled frequency scale.

Both the knowledge of the revealed series of discrete frequency bands in superconductor materials, realizing the currently developed laser technologies, that cover the entire EM spectrum, as well as the striking excitation/radiation semi-conductive features of smectites, could be applied to attain superconductive modes that finally may reach significant higher operation temperature levels.

Acknowledgement: We are indebted to Dr. Philip Turner for reading and studying several versions of our manuscript and providing us with welcome suggestions for improvement as well as complementary material for finalizing the present paper. We thank Trudi Sonderkamp for critical survey of the text and suggestions for improvement.

References

Alet F, Laflorencie N, Quantum simulation: Many-body localization: an introduction and selected topics. arXiv:1711.03145v2 [cond-mat.str-el], 2018.

Amiot E. The Torii of Phases. In: Yust J., Wild J., Burgoyne JA(eds) Mathematics and Computation in Music. MCM 2013. Lecture Notes in Computer Science, vol 7937. Springer, Berlin, Heidelberg.

Archilla JFR, Yu A. Kosevich N, Jiménez VJ, Sánchez-Morcillo, García-Raffi LM. Ultra discrete kinks with supersonic speed in a layered crystal with realistic potentials. Phys. Rev. E 91, 022912, 2015.

Archilla JFR, Palmero F, Lemos, CM, Sánchez-Rey B, Casado-Pascual J. Nonlinear systems. Vol. 2, Nonlinear phenomena in biology, optics and condensed matter, 2018, Publisher Cham, Switzerland: Springer.

Averkin AS et al., Superconductive ultra-compact magnetically coupled resonator with

twin-spiral structure. IEEE Transactions on Applied Superconductivity, 2017; https://arxiv.org/pdf/1412.5750.

Bardeen J, Cooper LN, Schrieffer JR. "Theory of superconductivity" Phys. Rev. 1957; vol. 108, pp. 1175–1204,http://link.aps.org/doi/10.1103/PhysRev.108.1175.

Bianconi A, Poccia N. Superstripes and Complexity in High-Temperature Superconductors, J. Supercon. Nov. Mag. 2012; DOI :10.1007/s10948-012-1670-6.

Bohm D. A Suggested Interpretation of the Quantum Theory in Terms of "Hidden" Variables, I & II. Physical Review 1952; 85, 166-179.

Borchardt GA. Montmorillonite and other smectites minerals, Minerals in soil environment. Soil Science Society of America, 1977.

Brizhik LS, Davydov AS. Fiz. Nizk., 1984; Temperatur 10, 358.

Byrnes T, Kim NY, Yamamoto Y. Exciton-polariton condensates, 2014; arXiv:1411.6822v1 [cond-mat.quant-gas].

Cavalleri A. Photo-induced superconductivity. Contemporary Physics, 2017; http://qcmd.mpsd.mpg.de/files/qcmd-theme/publications/2017/contphys2017-caval-phot-ind-sc.pdf.

Cavalleri A. Light induced superconducting-like properties in high-Tc cuprates, 2018; http://qcmd.mpsd.mpg.de/index.php/research/research-science/Light-induced-SC-like-properties-in-cuprates.html.

Cea, T, Barone P, Castellani C, Benfatto L. Polarization dependence of the third-harmonic generation in multiband superconductors. Phys. Rev. 2018; B 97, 094516.

Collini E, Wong CY, Wilk KE, Curmi PMG, Brumer P, Scholes GD. Coherently wired light-harvesting in photosynthetic marine algae at ambient temperature. Nature 2010; 463, 644–647.

Coyne LM. A possible energetic role of mineral surfaces in chemical evolution. Orig Life Evol Biosph. 1985;15:161–206.

Davydov AS. Solitons in Molecular Systems Phys. 1990; Rep. 190, 191. (Naukova Dumka, Kiev, 1988), in Russian.

Davydov AS, Ermakov VN. Stability of a Superconducting Condensate of Bisolitons, 1988; https://doi.org/10.1002/pssb.2221480128.

Dolce D. Introduction to the Quantum Theory of Elementary Cycles: The Emergence of Space, Time and Quantum. 2017; arXiv:1707.00677v1 [physics.gen-ph].

Dolce D, Perali A. The role of quantum recurrence in superconductivity, carbon nanotubes and related gauge symmetry breaking. Found Phys 2014; 44 905-922.

Engel, GS, Calhoun, TR, Read, EL, Ahn, T-K, Mancall, T, Cheng, Y-C, Blankenship, RE, Fleming, GR. Evidence for wavelike energy transfer through quantum coherence in photosynthetic systems. Nature 2007; **446**, 782–786

Ford PJ , Saunders GA. The Rise of the Superconductors. CRC Press Reference - 248 Pages - 85 B/W, 2004; ISBN 9780748407729 - CAT# TF2145.

Fripiat JJ. Application of far infrared spectroscopy to the study of clay minerals and zeolite: in Advanced Techniques for Clay Mineral Analysis, 1982; Elsevier, New York, 191-210.

Fröhlich H. Long-range coherence and energy storage in biological systems. Int. J. Quantum Chem. 1968; 2:641–649.

Geesink JH. Patent. Mineral composition, 2007; EP 1834926 A1, CN101400604A, EP1996513A1, US20090214659, WO2007101643A1.

Geesink JH and Meijer, DKF. Bio-Soliton Model that Predicts Non-Thermal Electromagnetic Frequency Bands, that Either Stabilize Living Cells. Electromagnetic Biology and Medicine, 2017a; 36, 357-378. https://doi.org/10.1080/15368378.2017.1389752.

Geesink JH and Meijer DKF. Electromagnetic Frequency Patterns that are Crucial for Health and Disease Reveal a Generalized Biophysical Principle: the GM scale. Quantum Biosystems, 2017b; 8, 1-16.

Geesink JH and Meijer DKF. Mathematical Structure of the GM Life Algorithm that May Reflect Bohm's Implicate Order. J. Modern Physics, 2018a; 9, 851- 897.

Geesink JH and Meijer DKF. A semi-harmonic electromagnetic frequency pattern organizes non-local states and quantum entanglement in both EPR studies and life systems. J. Modern Physics, 2018b; 9, 898-924.

Geesink JH and Meijer DKF. Semi-Harmonic Scaling enables Calculation of Masses of Elementary Particles of the Standard Model. J Modern Physics, 2018c; 9(5):925-947.

Geesink JH and Meijer, DKF Evidence for a Guiding Coherence Principle in Quantum Physics, Quantum Biosystems | 2018d | Vol 9 | Issue 1 | Page 1- 7.

Geesink JH and Meijer DKF. Electromagnetic frequencies of purified water show a coherent

GM-pattern that resembles that of life cells. In preparation., 2018e.

Germash KV, Fil DV. Strong enhancement of third-harmonic generation in a double layer graphene system caused by electron-hole pairing, EPL (Europhysics Letters), 2017; Volume 118, Number 6.

Gioacchino DD, Marcelli A, Puri A, Bianconi A. The a.c. susceptibility third harmonic component of NdO1-0.14F0.14FeAs: A flux dynamic magnetic analysis. Journal of Physics and Chemistry of Solids 71,2010; 1046–1052.

Horowitz GT. Introduction to Holographic Superconductors, 2010; arXiv:1002.1722 [hep-th]

Hu S, Kaiser, Nicoletti D, Hunt CR, Gierz I, Hoffmann MC, Le Tacon M, Loew T, Keimer B, Cavalleri A. Optically enhanced coherent transport in YBa2Cu3O6.5 by ultrafast redistribution of interlayer coupling. Nature Materials, 2014a; 13, 705–711

Huelga, SF and Plenio MB. Vibrations, Quanta and Biology. International Journal of Modern Physics B. 2013;10: 1735–1754 .

Jerman I. *The Origin of Life from Quantum Vacuum*, Water and Polar Molecules. American Journal of Modern Physics, 2016;5(4-1):34-43.

Kaiser S. et al. Optically induced coherent transport far above Tc in underdoped YBa2Cu3O6+δ. *Physical Review B* **89**, 2014; doi:10.1103/PhysRevB.89.184516.

Kavokin, A. Exciton-polaritons in microcavities: Recent discoveries and perspectives. Phys. Status Solidi B 2010; 247, 1898;1906.

Kennes, DM, Claassen M, Sentef MA, Karrasch C. Light-induced d-wave superconductivity, 2018; arXiv:1808.04655v1 [cond-mat.str-el].

Keppler JA. On the universal mechanism underlying conscious systems and the foundations for a theory of mind. Open J. of Philosophy 2016; 6: 346-367.

Kruchinin SP. Multiband Superconductors. Reviews in Theoretical Science 2016; Vol. 4, pp. 1–14.

Lane DA. Developing a Quantum Toolbox: Experiments with a Single-Atom Harmonic Oscillator and Prospects for Probing Molecular Ions, thesis, 2017.

Laughlin RB. A different Universe: Reinventing Physics from the Bottom Down, Basic books, 2005.

Mourachkine A. ROOM-TEMPERATURE SUPERCONDUCTIVITY, Book Cambridge International Science Publishing 7 Meadow Walk, Great Abington, Cambridge CB1 6AZ, UK http://www.cisp-publishing.com First published 2004.

Meijer DKF. The Extended Brain: Cyclic Information Flow, in a Quantum Physical Realm. NeuroQuantology, 2014; vol. 12, pp 180-200. http://www.neuroquantology.com/index.php/journal/article/view/754/651.

Meijer DKF. The Universe as a Cyclic Organized Information System. An Essay on the Worldview of John Wheeler. NeuroQuantology, 2015; 1, pp 1-40, http://www.neuroquantology.com/index.php/journal/article/view/798/693

Meijer DKF and Geesink JH. Phonon Guided Biology. Architecture of Life and Conscious Perception are mediated by Toroidal Coupling of Phonon, Photon and Electron Information Fluxes at Discrete Eigenfrequencies. NeuroQuantology, 2016; vol.14, issue 4: pp 718-755 http://www.neuroquantology.com/index.php/journal/article/view/985.

Meijer DKF and Geesink JH. Consciousness in the Universe is Scale Invariant and Implies *the Event Horizon of the Human Brain.* NeuroQuantology, 2017; 15, 41-79. https://www.neuroquantology.com/index.php/journal/article/viewFile/1079/852

Meijer and Geesink. Is the Fabric of Reality Guided by a Semi-Harmonic, Toroidal Background Field? International Journal of Structural and Computational Biology, Symbiosis, 2018a.

Meijer DKF and Geesink JH. Guided folding of life's proteins in integrate cells with holographic memory and GM-biophysical steering. Open Journal Of Biophysics, 2018b, 8(3):117-154.

Melkikh AV and Meijer DKF. On a generalized Levinthal's paradox: the role of long- and short range interactions on complex bio-molecular reactions, including protein and DNA folding. Progress in Biophysics and Molecular Biology, 2018;132:57-79. doi: 10.1016/j. pbiomolbio.2017.09.018.

Mitrano M. et al. Possible light-induced superconductivity in K3C60 at high temperature, *Nature*, *2016;*. DOI: 10.1038/nature16522.

Nicoletti D, Fu D, Mehio O, Moore S, Disa AS, G GD, Cavalleri A. Magnetic-field tuning of photo-induced superconductivity in striped La2-xBaxCuO4, 2018*;* ttps://arxiv.org/ftp/arxiv/papers/1803/1803.05420.pdf.

Okamoto J, Hu, W, Cavalleri A, Mathey l. Transiently enhanced interlayer tunneling in optically driven high-Tc superconductors. Physical Review B, 2017; v. 96, Issue 14,

https://doi.org/10.1103/PhysRevB.96.144505 https://hdl.handle.net/2144/31458.

Peng F , Sun Y, Pickard CJ, Needs RJ, Wu Q, Ma Y. Hydrogen Clathrate Structures in Rare Earth Hydrides at High Pressures: Possible Enroute to Room-temperature Superconductivity, 2017;PACS numbers: 74.70.Ad, 74.10.+v, 74.25.Jb, 74.62.Fj.

Plenio MB and Huelga SF. *Dephasing-assisted transport: quantum networks and biomolecules*. New J Physics, 2008; 10, 113019.

Poccia, N, Ricci, A, Bianconi, A. Fractal structure favouring superconductivity at high temperatures in a stack of membranes near a strain quantum critical point. J. Supercond. Nov. Magn. 2011a; 24, 1195–1200.

Poccia N. and Bianconi A. Meeting Report The Physics of Life and Quantum Complex Matter: A Case of Cross-Fertilization Life 1, 3-6; 2011b; doi:10.3390/life1010003 life ISSN 2075-1729 www.mdpi.com/journal/life.

Roushan P. et al. Spectral signatures of many-body localization with interacting photons, 2017; arXiv:1709.07108v2 [quant-ph].

Rajasekaran SJ, Okamoto L, Mathey M, Fechner V, Thampy, Gu GD, Cavalleri A. Probing optically silent superfluid stripes in cuprates. Rajasekaran et al., Science 2018; 359, 575–579.

Rezzolla L, Yoshida S, Maccarone TJ, Zanotti O. A new simple model for high-frequency quasi-periodic oscillations in black hole candidates. Monthly Notices of the Royal Astronomical Society, 2003; 344(3):L37-L41.

Romero E, Augulis R, Novoderezhkin VI, Ferretti M, Thieme J, Zigmantas D, Grondelle R. Quantum coherence in photosynthesis for efficient solar-energy conversion. Nat. Phys.**10**, 676–682.

Rong-Gen C A I, Li Li, Li-Fang L I, YangQui Y, 2015. Introduction to holographic superconductor models. Science China, Physics, Mechanics & Astronomy 2014; 58, 060401.

Sepehri A, Pincak R. Olmo GJ. M-theory-branes and superconductive wormholes. Int. J. of Geometric Methods in Modern Physics, 2017;14, 1-32.

Simpson WMR. Surprises in theoretical casimir physics: quantum forces in inhomogeneous media, 2015; https://www.springer.com/la/book/9783319093147.

Tranquada J. Hidden superconductivity revealed. Kathryn Allen, Materials World magazine, 2018.

'tHooft, G. Mathematical Theory for a Deterministic Quantum Mechanics. Journal of Physics, 2007; Conference Series.

'tHooft, G. Fundamental Theories of Physics, The Cellular Automaton Interpretation of Quantum Mechanics. 2016;185.

Tranter GE. Parity-violating energy differences of chiral minerals and the origin of biomolecular homochirality. Nature volume, 1985; 318, pages 172–173.

Turner P and Nottale L. The origins of macroscopic quantum coherence in high temperature superconductivity, 2015; arXiv:1410.3659v5.

Turner P and Notalle, L. A New Ab Initio Approach to the Development of High Temperature Superconducting Materials, J Supercond Nov Magn, 2016a; DOI 10.1007/s10948-016-3756-z.

Turner P and Notalle L. The physical principles underpinning self-organization on plants, 2016b; https://arxiv.org/pdf/160b2.08489.pdf

Vasconcellos AR, Vannuchi FS, Mascarenhas S, Luzzi R. Fröhlich. Condensate: Emergence of synergetic Dissipative Structures in Information Processing Biological and Condensed Matter Systems, Information, 2012.

Vattay G, Salahub D, Csabai I, Nassimi, A, Kaufmann SA. Quantum criticality at the origin of life. arXiv:1502.06880v2, 2015.

Zaanen JA. A modern, but way too short history of the theory of superconductivity at a high temperature, 2011; arXiv:1012.5461v2 [cond-mat.supr-con] 4 Jan.

Zurek WH. DECOHERENCE,EINSELECTION, AND THE EXISTENTIAL INTERPRETATION. Theoretical Astrophysics T-6, MS B288, LANL Los Alamos, New Mexico 87545 February 1, 2008; arXiv:quant-ph/9805065 865 (2017) 012007 doi :10.1088/1742-6596/865/1/012007.

Appendix 1. Periodic table of superconducting elements

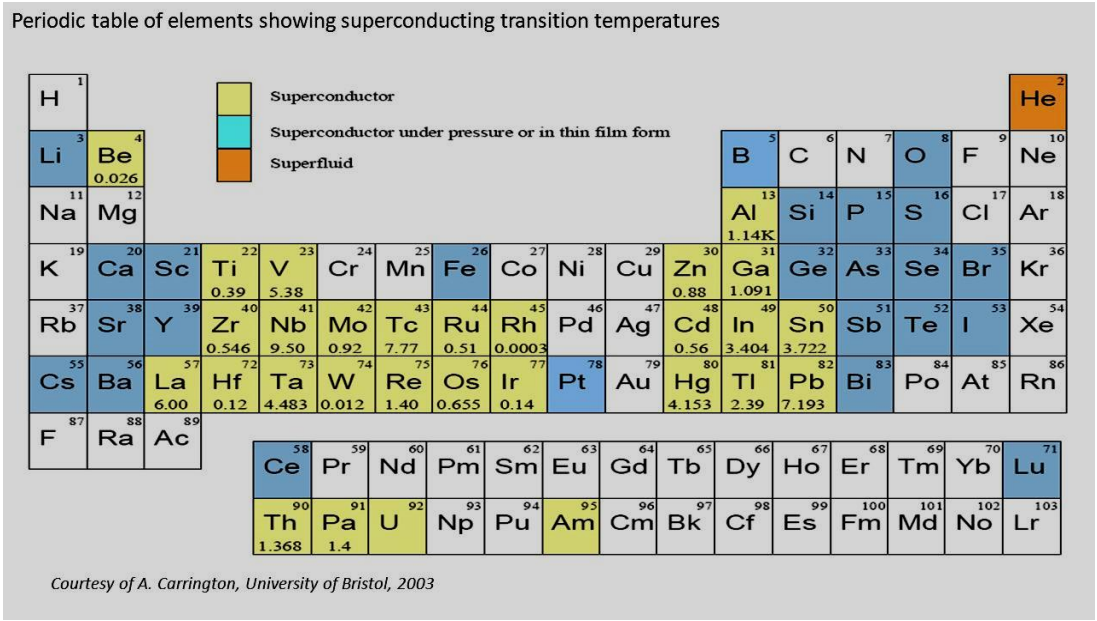

Periodic table of superconducting bulk elemental solids. Courtesy University of Bristol, 2003

Appendix 2. Calculated examples of coherent frequencies from sub Hertz till PHz

Factor	F1,m	F2,m	F3,m	F4,m	F5,m	F6,m	F7,m	F8,m	F9,m	F10,m	F11,m	F12,m
m=0	1.0000	1.0535	1.1250	1.1852	1.2656	1.3333	1.4142	1.5000	1.5803	1.6875	1.7778	1.8984 Hz
m=1	2.0000	2.1070	2.2500	2.3704	2.5312	2.6666	2.8284	3.0000	3.1606	3.3750	3.5556	3.7968 Hz
m=2	4.0000	4.2140	4.5000	4.7408	5.0624	5.3332	5.6568	6.0000	6.3212	6.7500	7.1112	7.5936 Hz
m=5	32.000	33.712	36.000	37.9264	40.4992	42.6656	45.2544	48.000	50.5696	54.000	56.8896	60.7488 Hz
m=8	256.00	269.70	288.00	303.41	324.00	341.33	362.04	384.00	404.54	432.00	455.12	486.00 Hz
m=12	4.0960	4.3151	4.6080	4.8546	5.1839	5.4613	5.7926	6.1440	6.4729	6.9120	7.2819	7.7759 KHz
2^24	16.777	17.675	18.874	19.884	21.233	22.370	23.726	25.166	26.513	28.312	29.827	31.850 MHz
2^32	4.2950	4.5248	4.8318	5.0904	5.4357	5.7266	6.0739	6.4425	6.7873	7.2478	7.6356	8.1536 GHz
2^40	1.0995	1.1583	1.2370	1.3031	1.3915	1.4660	1.5549	1.6493	1.7376	1.8554	1.9547	2.0873 Thz
2^48	281.47	296.53	316.66	333.60	356.23	375.29	398.06	422.21	444.81	474.99	500.41	534.35 Thz

532.5	505.6	473.4	449.3	420.8	399.5	376.6	710.1	674.0	631.3	599.1	561.0 nm

Appendix 3. The different analyzed superconductors and a semiconductor

Cuprates: $Bi_2Sr_2Ca_2Cu_3O_{10}$, $Y_{1.2}Ba_{0.8}CuO_{4-y}$; $(La_{1-x}Sr_x)_2CuO_4$, $YBa_2Cu_3O_{6.95}$, $YBa_2Cu_3O_7$ d (Y123), $YBa_2Cu_3O_{6+x}$, $YBa_2Cu_3O_{7-\delta}$, $Tl_2Ba_2CaCu_2O_8$, $Bi_2Sr_2CaCu_2O_{8+d}$, $La_{1.895}Sr_{0.105}CuO_4$, Nd-Ce-Cu-O, $Bi_2Sr_2CaCu_{208}$, $Bi_2Sr_{1.6}La_{0.4}CuO_{6+\delta}$, $MBa_2Cu_3O_7$ (M = Y, Sm, Eu, Gd, Ho, Nd, Dy, Er, Tm).
Pnictides and iron-based superconductors: $Nb\text{-}In_{0.75}Ga_{0.25}As\text{-}Nb$, $LaFeAsO_{0.87}F_{0.13}$, $LaFeAsO_{0.87}F_{0.13}$, $FeTe_{0.6}Se_{0.4}$, (La,Eu)FeAsO, $NdFeAsO_{0.6}F_{0.4}$, FeSe, Ferromagnetic Nanodiamond.
Superconductors containing aluminum: $Nb\text{-}AlO_x$ -Nb, $Mg_{1-x}Al_xB_2$, High-Q Aluminum (3D).
Metals and alloys: Nb, NbTiN, MoN, InSb, InAs, ZrB_{12}, YPtBi, HoPdBi, $LuNi_2$ B_2 C, YNi_2B_2C.
Other superconductors: Si/Ge, GeH_4, H_3S, CaC_6, doped-2$(Si,Al)_4O_{10}(OH)_{2-x}H_2O$, $ErNi_{211}B_2C$, $LuNi_2B_2C$, $Na_xCoO_{2.y}H_2O$, $BaPb_{1-x}Bi_xO_3$, $Ba_{06}K_{04}BiO_3$, $Na_2Ti_2Sb_2O$, $NdO_{0.3}F_{0.7}BiS_2$, Nitrogen vacancy diamond hybrid, Rare-earth borocarbides, Silicene, Actinium hydrides, Graphene.

Authors, year and labels used in figure 10

Shi 2008 (1), Kouwenhoven 2017, 2018 (2a, 2b, 2c), Cardona 1987 (3), Cardona 1988 (4a, 4b), Thakur 2013 (5), Mohan 2006 (6a, 6b), Renk 1987 (7), Sugai 1987 (8), Xianyu 1990 (9), Ravindran 2003 (10), Kawano 1996 (11), Kawano-Furukawa 2002 (12a, 12b), Pickett 1994 (13), Zibold 1998 (14), Kadowaki 2008 (15a, 15b, 15c), Tafuri 2016 (16a, 16b), Homes 2000 (17), Paik 2011 (18), Reagor 2013 (19a, 19b), Geesink (2013) (20a, 20b, 20c, 20d, 20e, 20f, 20g, 20h, 20i), Kaiser 2012 (21a, 21b), Tan 2015 (22), Jin 2010 (23a, 23b), Qiu 2008 (24a, 24b), Zhou 2016 (25), Delfanazari 2018 (26), Bruér 2016 (27), Wei 2008, (28a, 28b), Okazaki 2014 (29), Jha 2014 (30), Bobrov 2006 (31a, 31b), Szczesniak 2015 (32), Chen 2013 (33), Ichimura 2008 (34), Saito 2012 (35a, 35b), Zhu 2013 (36), Jünger 2016 (37), Zhang 2017 (38), Charnukha 2015 (39), Shi 2008 (40), Schlesinger 1989 (41), Chen 1999 (42), Malaeb 2017 (43), Hong 2013 (44), Hüfner 2008 (45a, 45b), Li 2002 (46), Kim 2018 (47), Pavlosiuk 2015 (48), Semenok 2018 (49a, 49b, 49 c, 49 d, 49 e, 49 f, 49 g), Szczęśniak 2015 (50), Durajski (51a, 51b, 51c), Groll 2014 (52a, 52b), Sprau 2017 (53a, 53b), Nicoletti, 2017 (54a, 54b), Capitani, 2017 (55). Kizilaslan, 2017 (56). Ludbrook, Graphene, 2015 (57). Manaf, Twisted Graphene, 2015 (58).

Table 1. The different Superconductors

1. $NaxCO_{02.y}H_2O$, Shi
2. InSb and InAs Nanowire Networks, Kouwenhoven
3. $MBa_2Cu_3O_7$ (M = Y, Sm, Eu, Gd, Ho), Cardona
4. $MBa_2Cu_3O_7$ (M =Nd, Dy, Er, Tm), Cardona
5. ZrB_{12}, Thakur
6. $Bi_2Sr_2Ca_2Cu_3O_{10}$, Mohan
7. Y1.2Ba0.8CuO4-y, Renk
8. $(La_{1-x}Srx)_2CuO_4$, Sugai
9. Nd-Ce-Cu-O system, Xianyu
10. Rare-earth transition-metal Borocarbides, Ravindran
11. YNi_2B_2C, Kawano
12. $ErNi_{211}B_2C$, Kawano
13. $LuNi_2B_2C$, Pickett
14. $Tl_2Ba_2CaCu_2O_8$, Zibold
15. $Bi_2Sr_2CaCu_2O_{8+d}$, Kadowaki
16. $Nb\text{-}AlO_x$ -Nb, Tafuri
17. Homes, doped $YBa_2Cu_3O_{6.95}$
18. High-Q Aluminum Superconducting (3D), Paik
19. Aluminum Cavities, Reagor
20. Multiband $2(Si, Al)_4O_{10}(OH)_2$ - xH_2O, Geesink
21. YBa_2Cu_{3O6+x}, Kaiser
22. Oxypnictide $Na_2Ti_2Sb_2O$, Tan
23. Niobium film, Jin
24. Oxypnictide $LaFeAsO_{0.87}F_{0.13}$, Qiu
25. FeSe on $SrTiO_{3(110)}$, Zhou
26. $Nb\text{-}In_{0.75}Ga_{0.25}As\text{-}Nb$, Delfanazari
27. Bruér $YBa_2Cu_3O_{7-\delta}$
28. $Bi_2Sr_{1.6}La_{0.4}CuO_{6+\delta}$, Wei
29. $FeTe_{0.6}Se_{0.4}$, Okazaki
30. $NdO_{0.3}F_{0.7}BiS_2$, Jha
31. $LuNi_2B_2C$, Bobrov
32. CaC_6, Szczesniak
33. Silicene, Chen
34. $LaFeAsO_{1-x}F_x$ (x =0.07), Ichimura
35. Nitrogen vacancy diamond hybrid system, Saito
36. Nitrogen vacancy diamond hybrid, Zhu
37. Si/Ge Nanowire, Jünger
38. Ferromagnetic Nanodiamond, Zhang
39. $NdFeAsO_{0.6}F_{0.4}$, Charnukha
40. $La_{1.895}Sr_{0.105}CuO_4$, Shi
41. $Ba_{06}K_{04}BiO_3$, Schlesinger
42. Nb/AlOx/Nb, Chen
43. (La,Eu)FeAsO, Malaeb
44. NbTiN, Hong
45. $Bi_2Sr_2CaCu_2O_{8+\delta}$, Hüfner
46. $YBa_2Cu_3O_7$ d (Y123), Li,
47. YPtBi, Kim
48. HoPdBi, Pavlosiuk
49. Actinium hydrides, Semenok
50. Germane (GeH_4), Szcz,e´sniak
51. H_3S, Durajski
52. MoN and NbTiN thin films, Groll
53. FeSe, Sprau
54. $BaPb_{1-x}Bi_{x03}$, Nicoletti
55. H_3S, Capitani
56. $Bi_2Sr_2CaCu_2O_{8+d}$, Kizilaslan
57. Graphene, Ludbrook.
58. Twisted Graphene, Manaf

Table 2. Calculated Reference spectral energy gaps of superconducting materials

1) Shi, NaxCoO2.yH2O; 19.90 THz, norm. 1.244 THz, delta 0.55%
2) Kouwenhoven, InSb and InAs Nanowire Networks:
2a) 0.15717 Thz , norm. 1.257 THz, delta 1.67%
2b) 0.18135 Thz, norm. 1.451 THz, delta 1.04%
2c) 0.21762 Thz , norm. 1.741 THz, delta 0.19%
2d) 0.09672 THz, norm 1.548 Thz, delta 0.48%
3) Cardona, $MBa_2Cu_3O_7$ (M = Y, Sm, Eu, Gd, Ho); 1.5739 Thz, norm. 1.574 THz, delta 0.93%
4) Cardona, $MBa_2Cu_3O_7$ (M =Nd, Dy, Er, Tm);
4a) 9.29357 THz , norm. 1.162 THz, delta 0.29%
4b) 1. 8.39419 THz, norm. 2.099 THz, delta 0.54%
5) Thakur, ZrB_{12}; 1.76513 THz, norm. 1.7651 THz, Delta 1.58%
6) Mohan, $Bi_2Sr_2Ca_2Cu_3O10_{10}$:
6a) 18.317 THz, norm. 1.1448 THz, delta 1.17%
6b) 14.8397 THz, norm. 1.8550 THz, delta 0.02%
7) Renk, $Y_{1.2}Ba_{0.8}CuO_{4-y}$, (mixed phase), 6.59543 THz, norm. 1.649 Thz, Delta 0.03%
8) Sugai, $(La_{1-x}Srx)2CuO4$, 7.375 THz, norm. 1.844 Thz, delta 0.63%
9) Xianyu, Nd-Ce-Cu-O system, 27.281 THz, norm. 1.705 THz, delta 1.88%
10) Ravindran, Rare-earth transition-metal borocarbides, 24.883 THz, norm. 1.555 THz, delta 0.02%
11) Kawano, YNi_2B_2C, 0.96720 THz, norm. 1.934 THz, delta 1.04%
12) Kawano-Furukawa, $ErNi_2{}^{11}B_2C$:
12a) 1.45 THz, norm. 1.45 THz, delta 1.09%
12b) 0.967 THz, norm. 1.934 Thz, delta 1.06%
13) Pickett, LuNi2B2C, 4.3470 THz, norm. 1.0868 Thz, delta 1.16%
14) Zibold, Tl2Ba2CaCu2O8, 29.979 THz, norm. 1.874 Thz , delta 0.98%
15) Kadowaki Bi2Sr2CaCu2O8+d:
15a) 1.296 Thz, norm. 1.296 Thz, Delta 0.55%
15b) 1.3031 THz, norm. 1.3031 Thz , delta 0.506%;
15c) 1 .64825 THz, norm. 1.6483 Thz , delta 0.55%
16) Tafuri, Nb-AlOx -Nb
16a) 5.11 THz, norm. 1.278 Thz, delta 0.39%
16b) 1.245 THz, norm. 1.245 THz, delta 0.62%
17) Homes, doped YBa2Cu3O6.95, 66.49471 Thz, norm. 2.078 Thz, delta 0.45%
18) Paik, High-Q Aluminum Superconducting (3D), 11.42 Ghz 1.4617 Thz, delta 0.29%
19) Reagor, Aluminum Cavities:
19a) 7.69 GHz, norm.1.969 Thz, delta 0.71%
19b) 11.4 GHz, norm. 1.459 Thz, delta 0.46%
20) Geesink, multiband 2(Si, Al)4O10(OH)2 - xH2O:
20a) norm. 1.11 THz, delta 0.96%
20b) norm. 1.233 THz, delta 0.32%
20c) norm. 1.315 THz, delta 0.91%
20d) norm. 1.39 THz, delta 0.11%
20e) norm. 1.47 THz, delta 0.27%
20f) norm. 1.65 THz, delta 0.04%
20g) norm. 1.73 THz, delta 0.44%
20h) norm. 1.94 Thz, delta 0.75%
20i) norm. 2.095 THz, delta 0.37%
21) Kaiser, YBa2Cu3O6+x
21a) 20 Thz, norm. 1.250 Thz, delta 1.06%
21b) 800-nm, norm. 1.468 Thz, delta 0.125%
22) Tan, Oxypnictide Na2Ti2Sb2O, 15.7 Thz, norm. 1.9625 Thz, delta 0.40%
23) Jin, Niobium film:
23a) 0.132 THz, norm. 2.112 Thz, delta 1.18%
23b) 0.418 THz, norm. 1.672 THz, delta 1.38%
24) Qiu, LaFeAsO0.87F0.13:
24a) 2.9 THz, norm. 1.450 Thz, delta 1.09%
24b) 4.11 THz, norm. 2.0550 THz, delta 1.55%
25) Zhou, FeSe on SrTiO3(110), 4.1106 THz, norm. 2.0553 THz, delta 1.55%
26) Delfanazari, Nb-In0.75Ga0.25As-Nb, 0.15717 THz, norm.1.257 THz, delta 1.54%
27) Bruér, YBa2Cu3O7−δ, 4.1589 THz, norm. 2.0795 THz delta 0.37%
28) Wei, Bi2Sr1.6La0.4CuO6+δ:
28a) 4.594 THz, norm.1.149 TH, delta 0.85%
28b) 8.22 THz, norm. 2.055 THz, delta 1.55%
29) Okazaki, FeTe0.6Se0.4, 0.29 THz, norm, 1.160 Thz, delta 0.15%
30) Jha, NdO0.3F0.7BiS2, 14.9 THz, norm. 1.863 Thz, delta 0.38%
31) Bobrov, $LuNi_2B_2C$:
31a) 0.5223 THz, norm. 2.089 Thz, delta 0.07%
31b) 0.4690 THz, norm. 1.876 THz, delta 1.11%
32) Szczesniak, CaC6, 44.346 THz, norm. 1.386 THz, delta 0.41%
33) Chen, Silicene, 8.46296 THz, norm. 2.116 THz, 1.36% som 21.4
34) Ichimura, LaFeAsO 1- x F x (x =0.07), 1.4508 THz, norm. 1.451 THz, 1.04%
35) Saito, Diamond hybrid system:
35a) 2.88 GHz, norm. 1.475 THz, delta 0.58%
35b) 638 nm, 469.894 THz, norm. 1.8355 Thz delta 0.74%
36) Zhu, nitrogen vacancy diamond hybrid, 2.878 GHz, norm. 1.474 THz, delta 0.51%
37) Jünger, Si/Ge Nanowire, 0.6529 THz, norm. 1.3058 THz, delta 0.2%
38)Zhang, Ferromagnetic Nanodiamond, 1.45 mev, 1.4024 THz, delta 0.79%
39) Charnukha, NdFeAsO0.6F0.4, 2.5389 THz, norm. 1.269 THz, delta 2.62%
40) Shi, La1.895Sr0.105CuO4, 6.28677 THz, norm. 1.572 THz, delta 1.08%
41) Schlesinger, Ba06K04BiO3, 149.8962 THz, norm. 1.1711 Thz, delta 1.10 %
42) Chen, Nb/AlOx/Nb, Chen, 770 GHz, norm. 1.540 THz, delta 0.96%
43) Malaeb, (La,Eu)FeAsO, 9.91376 THz, norm. 1.239 THz, delta 0.18%
44) Hong, NbTiN, 8.82566 Thz, norm. 1.1032 THz delta 0.34%
45) Hüfner, Bi2Sr2CaCu2O8+δ:
45a) 18.37672 Thz, norm. 1.1486 THz delta 0.84%

45b) 9.91376 THz, norm 1.2392 THz delta 0.18%
46) Li, Mg1−xAlxB2, 28.2 THz, norm. 1.7625 THz, delta 1.43%
47) Kim, YPtBi, 8.46296 Thz, norm 2.1157 THz, delta 1.36%
48) Pavlosiuk, HoPdBi, 15.47513 Thz, norm. 1.9344 Thz, delta 1.04%
49) Semenok, Different Actinium hydrides:
49a) 7 THz, norm. 1.75 Thz, delta 0.71%
49b) 7.5 THz, norm. 1.875 THz, delta 1.06%
49c) 31 Thz, norm. 1.9375 THz, delta 0.88%
49d) 35 Thz, norm. 1.0938, delta 0.52%
49e) 43 THz, norm. 1.3438 THz, delta 3.1%
49f) 50 THz, norm. 1.5625 Thz, delta 0.49%
49g) 59 THz, norm. 1.8438 THz, delta 0.63%
50) Szczęśniak, GeH4, 80.036 Thz, norm 1.251, THz delta 1.10 %
51) Durajski, H3S:
51a) 18.47344 Thz, norm. 1.1546 THz, delta 0.32%
51b) 23.01926 THz, norm. 1.4387 THz, delta 1.86 %
51c) 62.06979 THz, norm. 1.9397 THz delta 0.77%
52) Groll, MoN and NbTiN thin films:
52a) 0.48360 THz, norm. 1.9344 THz, delta 1.04%
52b) 0.58032 THz, norm. 1.1606 THz, delta 0.2%
53) Sprau FeSe:
53a) 0.556 THz, norm. 1.112 THz, delta 1.14%
53b) 0.363 THz, norm. 1.452 THz, delta 0.96%
54) Nicoletti, $BaPb_{1-x}BixO_3$:
54a) 375 THz, norm. 1.465 THz, delta 0.08%
54b) 60 THz, norm 1.875 Thz delta 1.06%

55) Capitani, H3S, 17.6513 THz, norm 1.1032 THz, delta 0.34%
56) Kizilaslan, Bi2Sr2CaCu2O8+d, 0.4836 THz, norm. 1.9344 Thz, delta 1.04%
57) Ludbrook, Graphene, 0.218 THz, norm. 1.7440 THz, delta 0.368%
58) Manaf, Twisted bilayer graphene, 1.451 THz, norm. 1.451 THZ, delta 1.09

Table 3. Literature references for calculation of the frequencies of the energy gaps of the different superconductors (at meV's, GHz, or THz)

1)M. Shi, J. Chang, S. Pailh´es, M. R. Norman, J. C. Campuzano,, M. M°ansson, T. Claesson, O. Tjernberg, A. Bendounan, L. Patthey, N. Momono, M. Oda, M. Ido, C. Mudry, and J. Mesot. The coherent d-wave superconducting gap in underdoped La2−xSrxCuO4 as studied by angle-resolved photoemission. arXiv:0708.2333v2 [cond-mat.supr-con] 27 Jul 2008.

2.1) Hao Zhang, Onder Gu, Sonia Conesa-Boj, Michał P. Nowak, Michael Wimmer, Kun Zuo, Vincent Mourik, Folkert K. de Vries, Jasper van Veen, Michiel W.A. de Moor, Jouri D.S. Bommer, David J. van Woerkom, Diana Car, Se´bastien R. Plissard, Erik P.A.M. Bakkers, Marina Quintero-Pe´rez, Maja C. Cassidy, Sebastian Koelling, Srijit Goswami, Kenji Watanabe, Takashi Taniguchi & Leo P. Kouwenhoven. Ballistic superconductivity in semiconductor nanowires. NATURE COMMUNICATIONS | 8:16025 |DOI: 10.1038/ncomms16025|, 2017.

2.2) Onder Gül, Hao Zhang, Jouri D.S. Bommer, Michiel W.A. de Moor, Diana Car, Sebastien R. Plissard, Erik P.A.M. Bakkers, Attila Geresdi, Kenji Watanabe, Takashi Taniguchi, Leo P. Kouwenhoven. Ballistic Majorana nanowire devices, arXiv:1603.04069v2 [cond-mat.mes-hall] 21 Dec 2017.

2.3) Folkert K. de Vries, Tom Timmerman, Viacheslav P. Ostroukh, Jasper van Veen, Arjan J. A. Beukman, Fanming Qu, Michael Wimmer, Binh-Minh Nguyen, Andrey A. Kiselev, Wei Yi, Marko Sokolich, Michael J. Manfra, Charles M. Marcus, and Leo P. Kouwenhoven. h/e Superconducting Quantum Interference through Trivial Edge States in InAs. Phys. Rev. Lett. 120, 047702 –26 January 2018.

3) M.Cardona, L. Genzel, R.Liu, A.Wittlin, H.J. Mattausch, F.García-Alvarado, E.García-González. Infrared and Raman spectra of the $MBa_2Cu_3O_7$-type high-Tc superconductors. Solid State Communications Volume 64, Issue 5, November 1987, Pages 727-732.

4) Cardona R, Liu C, Thomsen M, Bauer L, Genze, W, König A, Wittlin U, Amador M, Barahona F, Fernández C, Otero, R. Infrared and Raman spectra of the new superconducting cuprate perovskites $MBa_2Cu_3O_7$, M =Nd, Dy, Er, Tm. Solid State Communications Volume 65, Issue 1, January 1988, Pages 71-75.

5) Sangeeta Thakur, Deepnarayan Biswas, Nishaina Sahadev, P. K. Biswas, G. Balakrishnan, Kalobaran Maiti. Complex spectral evolution in a BCS superconductor, ZrB_{12}.
SCIENTIFIC REPORTS | 3 : 3342 | DOI: 10.1038/srep03342, 2013

6) S. Mohan, P. Murugesan, PHONON SPECTRA OF HIGH TEMPERATURE SUPERCONDUCTOR $Bi_2Sr_2Ca_2Cu_{3O}10_{10}$, Journal of Physical Science, Vol. 17(2), 51–66, 2006.

7) K. F. Renk, H. Lengfeliner, P. E. Obermayer, W. Ose, H. H. Otto, T. Zetterer. FAR INFRARED REFLECTANCE OF A MIXED PHASE, $Y_{1.2}Ba_{0.8}CuO_{4-y}$. International Journal of Infrared and Millimeter Waves, Vol. 8, No. 12, 1987.

8) Shunji Sugai, Shin-ichi Uchida, Hidenori Takagi, Koichi Kitazawa, Shoji Tanaka. Infrared Spectroscopy in High Tc Superconductors (La1-xSrx)2CuO4, Japanese Journal of Applied Physics, Volume 26, Part 2, Number 5, 1987.

9) Z. Xianyu, C.J.LiQ, L. Hu, J. H. Sun, W. Z., Wang, G.Yuan. Study of infrared spectra of N-type superconductor Nd-Ce-Cu-O system. Physica B: Condensed Matter, Volumes 165–166, Part 2, August 1990, Pages 1243-1244.

10) P.Ravindran, Raman- and infrared-active phonons in superconducting and non superconducting rare-earth transition-metal borocarbides, from full-potential calculations, 2003. PHYSICAL REVIEW B 67, 104507, 2003.
11) H. Kawano, H. Yoshizawa, H. Takeya, and K. Kadowaki, Anomalous Phonon Scattering Below Tc in YNi_2B_2C, Phys. Rev. Lett. 77, 4628 – Published 25 November 1996.
12) H. Kawano-Furukawa, H. Yoshizawa, H. Takeya, K. Kadowaki, Anomalous phonon peak in the superconducting state of $ErNi_2{}^{11}B_2C$, PHYSICAL REVIEW B 66, 212503, 2002.
13) Pickett WE, Singh DJ. LuNi2B2C: A novel Ni-based strong-coupling superconductor. Phys Rev Lett. 1994 Jun 6;72(23):3702-3705.PMID: 10056268 DOI: 10.1103/PhysRevLett.72.3702.
14) Axel M. Zibold, David B.Tanner, Helmuth Berger. Far-infrared study of superconducting Tl2Ba2CaCu2O8. Physica B: Condensed Matter Volume 244, 1 January 1998, Pages 27-32.
15) K. Kadowaki , H. Yamaguchi, K. Kawamata, T. Yamamoto, H. Minami, I. Kakeya, U. Welp, L. Ozyuzer, A. Koshele, C. Kurter, K.E. Gray, W.-K. Kwok. Direct observation of tetrahertz electromagnetic waves emitted from intrinsic Josephson junctions in single crystalline Bi2Sr2CaCu2O8+d , Physica C 468 (2008) 634–639, doi:10.1016/j.physc.2007.11.090.
16) Francesco Tafuri, Halima Giovanna Ahmad. Physics of the Josephson effect in junctions with ferromagnetic barrier. A.A. 2016/2017.
17) C. C. Homes, A. W. McConnell, B. P. Clayman, D. A. Bonn, Ruixing Liang, W. N. Hardy, M. Inoue, H. Negishi, P. Fournier, R. L. Greene. Phonon Screening in High-Temperature Superconductors, VOLUME 84, NUMBER 23 PHYSICAL REVIEW LETTERS 5 JUNE 2000.
18) Paik H. et al. Lecture Introducing 3D transmon. Phys. Rev. Lett. 107, 240501 (2011).
19) Matthew Reagor, Hanhee Paika), Gianluigi Catelanib), Luyan Sun, Christopher Axline, Eric Holland, Ioan M. Pop, Nicholas A. Maslukc), Teresa Brecht, Luigi Frunzio, Michel H. Devoret, Leonid Glazman, and Robert J. Schoelkopfd). Reaching 10 ms single photon lifetimes for superconducting aluminum cavities. Appl. Phys. Lett. 102, 192604 (2013); https://doi.org/10.1063/1.4807015.
20) Geesink, Mineral composition, Patent WO2007101643A1.
21) Kaiser, D. Nicoletti, C.R. Hunt, W. Hu, I. Gierz, H.Y. Liu, M. Le Tacon, T. Loew, D. Haug, B. Keimer, A. Cavalleri. Light-induced inhomogeneous superconductivity far above Tc in YBa2Cu3O6+x, DOI: 10.1103/PhysRevB.89.184516, 2012.
22) Tan S. Y. , J. Jiang, Z. R. Ye, X. H. Niu, Y. Song, C. L. Zhang, P. C. Dai, B. P. Xie, X. C. Lai and D. L. Feng. Photoemission study of the electronic structure and charge density waves of Na2Ti2Sb2O, Scientific Reports volume 5, Article number: 9515 (2015).
23) Jin B., Caihong Zhang, Sebastian Engelbrecht, Andrei Pimenov, Jingbo Wu, Qinyin Xu, Chunhai Cao, Jian Chen, Weiwei Xu, Lin Kang, and Peiheng Wu. Low loss and magnetic field-tunable superconducting terahertz metamaterial. Optics Express Vol. 18, Issue 16, pp. 17504-17509 (2010).
24) Qiu Y., M. Kofu, Wei Bao, S.-H. Lee, Q. Huang, T. Yildirim, J. R. D. Copley, J. W. Lynn, T. Wu, G. Wu, and X. H. Chen. Neutron-scattering study of the oxypnictide superconductor LaFeAsO0.87F0.13, Physical review. B, Condensed matter 78(5) · August 2008.
25) Zhou G., Ding Zhang, Chong Liu, Chenjia Tang, Xiaoxiao Wang, Zheng, Canli Song, Shuaihua, Ke He, Lili Wang, Xucun Ma, Qi-Kun Xue. Interface induced high temperature superconductivity in single unit-cell FeSe on SrTiO3(110). Appl. Phys. Lett. 108, 202603 (2016); https://doi.org/10.1063/1.4950964
26) Delfanazari, K and Puddy, R and Ma, P and Yi, T and Cao, M and Richardson, CL and Farrer, I and Ritchie, DA and Joyce, H and Kelly, M and Smith, CG (2018) On-chip hybrid superconducting-semiconducting quantum circuit. IEEE Transactions on Applied Superconductivity.
27) Bruér J., Ivan Maggio-Aprile, Nathan Jenkins, Zoran Ristić, Andreas Erb, Christophe Berthod, Øystein Fischer & Christoph Renner. Revisiting the vortex-core tunnelling spectroscopy in YBa2Cu3O7−δ Revisiting the vortex-core tunnelling spectroscopy in YBa2Cu3O7−δ. Nature Communications volume 7, Article number: 11139 (2016).
28) Wei, J., Y. Zhang, H. W. Ou, B. P. Xie, D. W. Shen, J. F. Zhao, L. X. Yang, M. Arita,K. Shimada, H. Namatame, M. Taniguchi, Y. Yoshida, H. Eisaki, and D. L. Feng1. Superconducting coherence peak in the electronic excitations of a single layer cuprate superconductor Bi2Sr1.6La0.4CuO6+δ. Physical Review Letters · August 2008. DOI: 10.1103/PhysRevLett.101.097005 · Source: PubMed.
29) Okazaki K. , Y. Ito, Y. Ota, Y. Kotani, T. Shimojima, T. Kiss, S. Watanabe, C.-T. Chen, S. Niitaka, T. Hanaguri, H. Takagi, A. Chainani & S. Shin. Superconductivity in an electron band just above the Fermi level: possible route to BCS-BEC superconductivity. SCIENTIFIC REPORTS | 4 : 4109 | DOI: 10.1038/srep04109, 2014.
30) Jha R., V P S Awana. Superconducting properties of BiS2 based superconductor NdO1-xFxBiS2 (x=0 to 0.9). Published 7 March 2014 • 2014 IOP Publishing Ltd Materials Research Express, Volume 1, Number 1.
31) Bobrov, N.L. ; Beloborod'ko, S.I. ; Tyutrina, L.V. ; Chernobay, V.N. ; Yanson, I.K. ; Naugle, D.G. ; Rathnayaka, K.D.D. Investigation of the superconducting energy gap in the compound

$LuNi_2$ B_2 C by the method of point contact spectroscopy: two-gap approximation. Experimental Methods and Applications, ACS:63.20.Kr, 72.10.Di, 73.40.Jn, 2006.

32) Szczęśniak R. , E. A. Drzazga1 and D. Szczęśniak. Isotropic and anisotropic description of superconducting state in CaC6 compound. Eur. Phys. J. B (2015) 88: 52 , https://doi.org/10.1140/epjb/e2015-50616-6.

33) Chen L. , Baojie Feng and Kehui Wu. Observation of superconductivity in silicene. Applied Physics Letters > Volume 102, Issue 8 > 10.1063/1.4793998, 2013.

34) Ichimura K., Junya Ishioka1, Toru Kurosawa2, Katsuhiko Inagaki1, Migaku Oda2, Satoshi Tanda. Superconducting Gap and Pseudogap Structure in LaFeAsO1-xFx Probed by STM/STS. J. Phys. Soc. Jpn. 77, pp. 151-152 (2008).

35) Shiro Saito, Xiaobo Zhu, William John Munro, and Kouichi Semba. Coherent Coupling between a Superconducting Qubit and a Spin Ensemble. NTT Technical Review, 2012.

36) Xiaobo Zhu, Yuichiro Matsuzaki , Robert Amsu¨ss, Kosuke Kakuyanagi, Takaaki Shimo-Oka, Norikazu Mizuochi, Kae Nemoto, Kouichi Semba, William J. Munro & Shiro Saito. Observation of dark states in a superconductor diamond quantum hybrid system. NATURE COMMUNICATIONS | 5:3524 | DOI: 10.1038/ncomms4524 www.nature.com/naturecommunications, 2013.

37) Christian Jünger, Semiconducting Nanowires with three superconducting contacts, lecture Si/Ge Nanowire with Aluminum contacts, www.nanoelectronics.ch, 2016.

38) Zhang G, Samuely T1, Xu Z2, Jochum JK, Volodin A, Zhou S3, May PW4, Onufriienko O1, Kačmarčík J1, Steele JA, Li J5, Vanacken J, Vacík J6, Szabó P1, Yuan H, Roeffaers MBJ, Cerbu D, Samuely P1, Hofkens J, Moshchalkov VV. Superconducting Ferromagnetic Nanodiamond. ACS Nano. 2017 Jun 27;11(6):5358-5366. doi: 10.1021/acsnano.7b01688. Epub 2017.

39) Charnukha A., D. V. Evtushinsky, C. E. Matt, N. Xu, M. Shi, B. Büchner, N. D. Zhigadlo, B. Batlogg & S. V. Borisenko. High-temperature superconductivity from fine-tuning of Fermi-surface singularities in iron oxypnictides. Scientific Reports | 5:18273 | DOI: 10.1038/srep18273, 2015.

40) Shi, J. Chang, S. Pailh´es, M. R. Norman, J. C. Campuzano,, M. M˚ansson, T. Claesson, O. Tjernberg, A. Bendounan, L. Patthey, N. Momono, M. Oda, M. Ido, C. Mudry, and J. Mesot. The coherent d-wave superconducting gap in underdoped La2−xSrxCuO4 as studied by angle-reolved photoemission, arXiv:0708.2333v2 [cond-mat.supr-con] 27 Jul 2008.

41) Schlesinger Z, Collins RT, Calise JA, Hinks DG, Mitchell AW, Zheng Y, Dabrowski B, Bickers NE, Scalapino DJ. Superconducting energy gap and a normal-state excitation in Ba0.6K0.4BiO3. Physical Review. B, Condensed matter 40(10):6862-6866 · November 1989.

42) V. Chen, A.V. Rylyakov, V. Patel, J.E. Lukens, and K.K. Likharev, "Rapid single flux quantum T flip-flop operating up to 770 GHz", IEEE Trans. on Appl. Supercond. vol. 1999.

43) Walid Malaeb, Ramadan Awad, Taku Hibino, Yoichi Kamihara, Takeshi Kondo, Shik Shin.Electronic structure of the iron-based superconductor (La,Eu)FeAsO1-xFx investigated by laser photoemission spectroscopy. JournalPhysica B: Condensed Matter, In press - 2017 Jun 30.

44) Hong T. , Kyujin Choi, Kyung Ik Sim, Taewoo Ha, Byung Cheol Park, Hirotake Yamamori, and Jae Hoon Kim. Terahertz electrodynamics and superconducting energy gap of NbTiN. Journal of Applied Physics 114, 243905 (2013); https://doi.org/10.1063/1.4856995.

45) S Hüfner, M A Hossain, A Damascelli and G A Sawatzky. Two gaps make a high-temperature superconductor? Rep. Prog. Phys. 71 (2008) 062501 (9pp) doi:10.1088/0034-4885/71/6/062501.

46) J. Q. Li, L. Li, F. M. Liu, C. Dong, J. Y. Xiang, and Z. X. Zhao. Superconductivity, superstructure, and structure anomalies in Mg1−xAlxB2, Phys. Rev. B 65, 132505 – Published 12 March 2002.

47) Kim H., Kefeng Wang, Yasuyuki Nakajima, Rongwei Hu, Steven Ziemak, Paul Syers, Limin Wang, Halyna Hodovanets, Jonathan D. Denlinger, Philip M. R. Brydon, Daniel F. Agterberg, Makariy A. Tanatar, Ruslan Prozorov and Johnpierre Paglione. Science Advances 06 Apr 2018: Vol. 4, no. 4, eaao4513, DOI: 10.1126/sciadv.aao4513.

48) Pavlosiuk O., Dariusz Kaczorowski, Xavier Fabreges, ArsenGukasov & PiotrWiśniewski. Antiferromagnetism and superconductivity in the half Heusler semimetal HoPdBi. Scientific Reports | 6:18797 | DOI: 10.1038/srep18797, 2015.

49) Semenok D.V., Alexander G. Kvashnin, Ivan A. Kruglov, Artem R. Oganov. Actinium Hydrides AcH10, AcH12, and AcH16 as High-Temperature Conventional Superconductors. J. Phys. Chem. Lett., 2018, 9 (8), pp 1920–1926. DOI: 10.1021/acs.jpclett.8b00615.

50) Szczęśniak, R. & Durajski, Detailed study of the superconducting properties in compressed germane. 2015. A. Eur. Phys. J. B (2015) 88: 342. https://doi.org/10.1140/epjb/e2015-60752-6.

51) Artur P. Durajski & Radosław Szczęśniak. First-principles study of superconducting hydrogen sulfide at pressure up to 500GPa. Scientific Reports | 7: 4473 | DOI:10.1038/s41598-017-04714-5.

52) Groll N.R., Jeffrey A. Klug, Chaoyue Cao, Serdar Altin, Helmut Claus, Nicholas G. Becker, John F. Zasadzinski, Michael J. Pellin, and Thomas Proslier. Tunneling spectroscopy of superconducting MoN and NbTiN grown by atomic layer deposition. Appl. Phys. Lett. 104,

092602 (2014); https://doi.org/10.1063/1.4867880.

53. Sprau, P.O., A. Kostin, A. Kreisel, A. E. Böhmer, Taufour, P. C. Canfield, S. Mukherjee,P. J. Hirschfeld, B. M. Andersen, J. C. Séamus Davis. Sprau et al., Discovery of orbital-selective Cooper pairing in FeSe. Science 357, 75–80 (2017) 7 July 2017.
54. Nicoletti D., E. Casandruc , D. Fu , P. Giraldo-Gallob, I. R. Fisher, A. Cavalleri, Anomalous relaxation kinetics and charge-densitywave correlations in underdoped BaPb1−xBixO3. 9020–9025 | PNAS | August 22, 2017 | vol. 114 | no. 34 www.pnas.org/cgi/doi/10.1073/pnas.1707079114.
55. Capitani, F., B. Langerome, J.-B. Brubach, P. Roy, A. Drozdov, M.I. Eremets, E. J. Nicol, J. P. Carbotte, T. Timusk. Spectroscopic evidence of a new energy scale for superconductivity in H3S. PublNat Phys. 2017 September ; 13(9): 859–863. doi:10.1038/nphys4156.
56. O. Kizilaslan, F. Rudau, R. Wieland, J.S. Hampp, X.J. Zhou, M. Ji, O. Kiselev, N. Kinev, Y. Huang, L.Y. Hao, A. Ishii, T. Hatano, V.P. Koshelets, P.H. Wu, H.B. Wang, D. Koelle, and R. Kleiner. Tuning THz emission properties of Bi2Sr2CaCu2O8+d intrinsic Josephson junction stacks by charge carrier injection», Superconductor Science and Technology, 30, 034006, January 2017; DOI: https://doi.org/10.1088/1361-6668/aa55ae.
57. Ludbrook, B.M., G. Levy, P. Nigge, M. Zonno, M. Schneider, D. J. Dvorak, C. N. Veenstra, S. Zhdanovich, D. Wong, P. Dosanj, C. Straßer, A. Stöhr, S. Forti, C. R. Ast, U. Starke, and A. Damascelli. Evidence for superconductivity in Li-decorated monolayer graphene, www.pnas.org/cgi/doi/10.1073/pnas.1510435112.
58. Muhamad Nasruddin Manaf, Iman Santoso, and Arief Hermanto. The possibility of superconductivity in twisted bilayer graphene AIP Conference Proceedings 1677, 070004 (2015); https://doi.org/10.1063/1.4930708.